# Tacrine-Xanomeline and Tacrine-Iperoxo hybrid ligands: Synthesis and biological evaluation at acetylcholinesterase and $M_1$ muscarinic acetylcholine receptors

Marco Maspero[a,1], Daniela Volpato[b,1], Davide Cirillo[a], Natalia Yuan Chen[b], Regina Messerer[b], Christoph Sotriffer[b], Marco De Amici[a], Ulrike Holzgrabe[b,*], Clelia Dallanoce [a,*]

[a] Department of Pharmaceutical Sciences, Medicinal Chemistry Section "Pietro Pratesi", University of Milan, Via L. Mangiagalli 25, 20133 Milan, Italy

[b] Pharmaceutical and Medicinal Chemistry, Institute of Pharmacy and Food Chemistry, University of Würzburg, Am Hubland, 97074 Würzburg, Germany

* Corresponding authors:

*E-mail addresses:* clelia.dallanoce@unimi.it (C. Dallanoce), ulrike.holzgrabe@uni-wuerzburg.de (U. Holzgrabe)

[1] These authors contributed equally to this work.

---

*Abbreviations:*

ACh, acetylcholine; AChE, acetylcholinesterase; AChEIs, acetylcholinesterase inhibitors; AD, Alzheimer's disease; ASP, Astex statistical potentials; ATC, acetylthiocholine iodide; BChE, butyrylcholinesterase; CAS, catalytic active site; CCh, carbachol; CHO, Chinese hamster ovary; CSD, Cambridge structural database; DAG, 1,2-diacylglycerol; DMEM, Dulbecco's modified Eagle's medium; DSX, DrugScoreX; DTNB, 5,5'-dithiobis-(2-nitrobenzoic acid); ELSD, evaporative light scattering detector; ESI, electrospray ionization; FCS, fetal calf serum; FRET, fluorescence resonance energy transfer; GDP, guanosine 5'-diphosphate; GTP, guanosine 5'-triphosphate; HAM- F12, Ham's nutrient mixture F-12; HBSS, Hank's balanced salt solution; HEPES, 4-(2-hydroxyethyl)-1-piperazineethanesulfonic acid; HepG2, human hepatocellular carcinoma; $hM_1R$, human $M_1$ receptor; HTRF, time-resolved fluorescence resonance energy transfer; IP1, inositol 1-phosphate; $IP_3$, inositol 1,4,5-trisphosphate; L-15, Leibovitz's L-15 medium; LC-MS, liquid chromatography mass spectrometry; mAChRs, muscarinic acetylcholine receptors; MOE, molecular operating environment; PAS, peripheral anionic site; PBS, phosphate-buffered saline; $PIP_2$, phosphatidylinositol 4,5-bisphosphate; PLC, phospholipase

C; PLCβ, phospholipase Cβ; RMSD, root-mean-square deviation; $R_f$, retention factor; CNS, central nervous system; TcAChE, *Torpedo californica* acetylcholinesterase.

ARTICLE INFO

*Keywords:*

Multitarget compounds

Bitopic ligands

Allosteric modulation

$M_1$ muscarinic acetylcholine receptor

Ellman's assay

Inositol monophosphate

Phospholipase C

Iperoxo

Tacrine

Xanomeline

A B S T R A C T

We synthesized a set of new hybrid derivatives (**7-C8**, **7-C10**, **7C12** and **8-C8**, **8-C10**, **8-C12**), in which a polymethylene spacer chain of variable length connected the pharmacophoric moiety of xanomeline, an $M_1/M_4$-preferring orthosteric muscarinic agonist, with that of tacrine, a well-known acetylcholinesterase (AChE) inhibitor able to allosterically modulate muscarinic acetylcholine receptors (mAChRs). When tested *in vitro* in a colorimetric assay for their ability to inhibit AChE, the new compounds showed higher or similar potency compared to that of tacrine. Docking analyses were performed on the most potent inhibitors in the series (**8-C8**, **8-C10**, **8-C12**) to rationalize their experimental inhibitory power against AChE. Next, we evaluated the signaling cascade at $M_1$ mAChRs by exploring the interaction of $G\alpha_q$-PLC-β3 proteins through split luciferase assays and the *myo*-Inositol 1 phosphate (IP1) accumulation in cells. The results were compared with those obtained on the known derivatives **6-C7** and **6-C10**, two quite potent AChE inhibitors in which tacrine is linked to iperoxo, an exceptionally potent muscarinic orthosteric activator. Interestingly, we found that **6-C7** and **6-C10** behaved as partial agonists of the $M_1$ mAChR, at variance with hybrids **7-Cn** and **8-Cn** containing xanomeline as the orthosteric molecular fragment, which were all unable to activate the receptor subtype response.

## 1. Introduction

The decrease in acetylcholine (ACh) levels as well as the dysfunction and decline of cholinergic neurons, which were the basis to formulate the "cholinergic hypothesis" of Alzheimer's disease (AD), are typical hallmarks associated with the neurodegenerative impairment of this pathology [1-3]. To improve the cholinergic neurotransmission, different approaches have been explored, including the enhancement of ACh synthesis, the augmentation of its presynaptic release, the stimulation of cholinergic postsynaptic muscarinic and nicotinic receptors, and the reduction of ACh synaptic degradation by means of cholinesterase inhibitors. Unfortunately, no resolution therapy for AD is currently available, and drugs on the market that inhibit acetylcholinesterase (AChEIs) are simply able to alleviate the disease symptoms and/or delay its progression.

Tacrine **1** (Fig. 1), the first AChEI approved by FDA for the AD therapy, was withdrawn from the market due to its dose-dependent hepatotoxicity [4]. Nevertheless, it still represents an interesting scaffold to be studied, since it positively modulates the affinity and functional response of ligands binding the orthosteric ACh site [5], showing some selectivity for the $M_1$ and $M_2$ mAChR subtypes [6]. Therefore, the molecular skeleton of tacrine has been used to develop a variety of hybrid molecules [3,7-11] with the purpose of combining the relevant AChE inhibition of the parental compound with other favorable pharmacological properties [12,13]. In addition, due to the ability of tacrine to occupy both the catalytic active site (CAS) and the peripheral anionic site (PAS) of the enzyme, bistacrine dimers like **2** (Fig. 1) showed a 1000-fold higher AChE inhibitory potency than tacrine itself [14].

As far as complementary or alternative approaches to the therapy of AD are considered, the current data do not support the application of orthosteric muscarinic agonists. In this respect, the most studied mAChR has been the $M_1$ subtype, which is widely expressed in the central nervous system

and is involved in many physiological and pathological brain functions as well as motor control and regulation of body temperature [15,16]. However, the orthosteric binding site of the $M_1$ receptor has high homology with the other mAChR subtypes, which results in pronounced side effects of the "selective" $M_1$ agonists developed so far [5]. On the other hand, the less conserved allosteric binding site of the $M_1$ receptor could be selectively targeted by allosteric $M_1$-selective enhancers, albeit to date compounds with this profile show comparatively weak potencies [17]. Among the investigated $M_1$ activators, xanomeline **3** (Fig. 1) is a $M_1/M_4$-preferring orthosteric agonist with promising antidementive properties *in vivo*, but its dose-limiting side effects precluded any clinical development [5,18]. Additionally, xanomeline has a peculiar mode of mAChR activation, being different from that of conventional agonists such as carbachol and endogenous ACh [19]. It was also reported to have a wash-persistent binding to the $M_1$ subtype, which may arise not only from hydrophobic interactions between the xanomeline's *O*-hexyl-containing chain and the receptor protein, but also from the ligand recognition of a secondary binding site on the receptor [20,21].

In this paper, we designed a new set of hybrid ligands containing the pharmacophoric moieties of tacrine and xanomeline, by exploiting our experience in the study of dualsteric (i.e. simultaneous orthosteric/allosteric) ligands [22-26] of mAChRs and hybrid derivatives active at the $M_1$ mAChR subtype as alleged antidementive agents [3,5,27,28] as well as with the purpose of developing new strategies for therapeutic intervention on AD. We aimed at multifunctional molecules combining synergistic effects. First, the direct activation of the $M_1$ receptor subtype at the orthosteric site by xanomeline, then AChE inhibition by the tacrine molecular portion coupled with a positive allosteric cooperativity between the two moieties at the examined receptor subtype. Hybrid compounds containing the same pharmacophoric fragments connected by various chemical spacers (amines **4** and amides **5**, Fig. 1) [5] showed a relevant AChE inhibition and a purely allosteric binding at the inactive $M_1$ mAChR, which precluded any activation of the receptor response.

Thus, we explored if a different molecular connection between the two pharmacophoric moieties could promote the expected pharmacological profile of the resulting hybrids, in particular their

behavior as $M_1$ mAChR activators. To such an end, in the designed compounds the primary amine group of tacrine was linked to the nitrogen atom of the tetrahydropyridine nucleus of xanomeline by means of alkyl chains of different length (Fig. 1). In this respect, we used as model compounds our prominent hybrid derivatives **6-C7**, **6-C10** (Fig.1) [3], in which tacrine was combined with the orthosteric muscarinic agonist iperoxo [29,30]. The new, putative bipharmacophoric ligands were prepared as tertiary amines **7-Cn** (**7-C8**, **7C-10**, **7-C12**) and their corresponding quaternary tetrahydropyridinium salts **8-Cn** (**8-C8**, **8-C10** and **8-C12**). All synthesized compounds were evaluated *in vitro* for their ability to inhibit AChE and activate $M_1$ receptors. To further investigate ligand-enzyme interactions, molecular modeling studies were also performed on the most potent inhibitors. For comparison, also hybrids **6-C7**, **6-C10** were evaluated for $M_1$ receptor activation, revealing a promising biological profile.

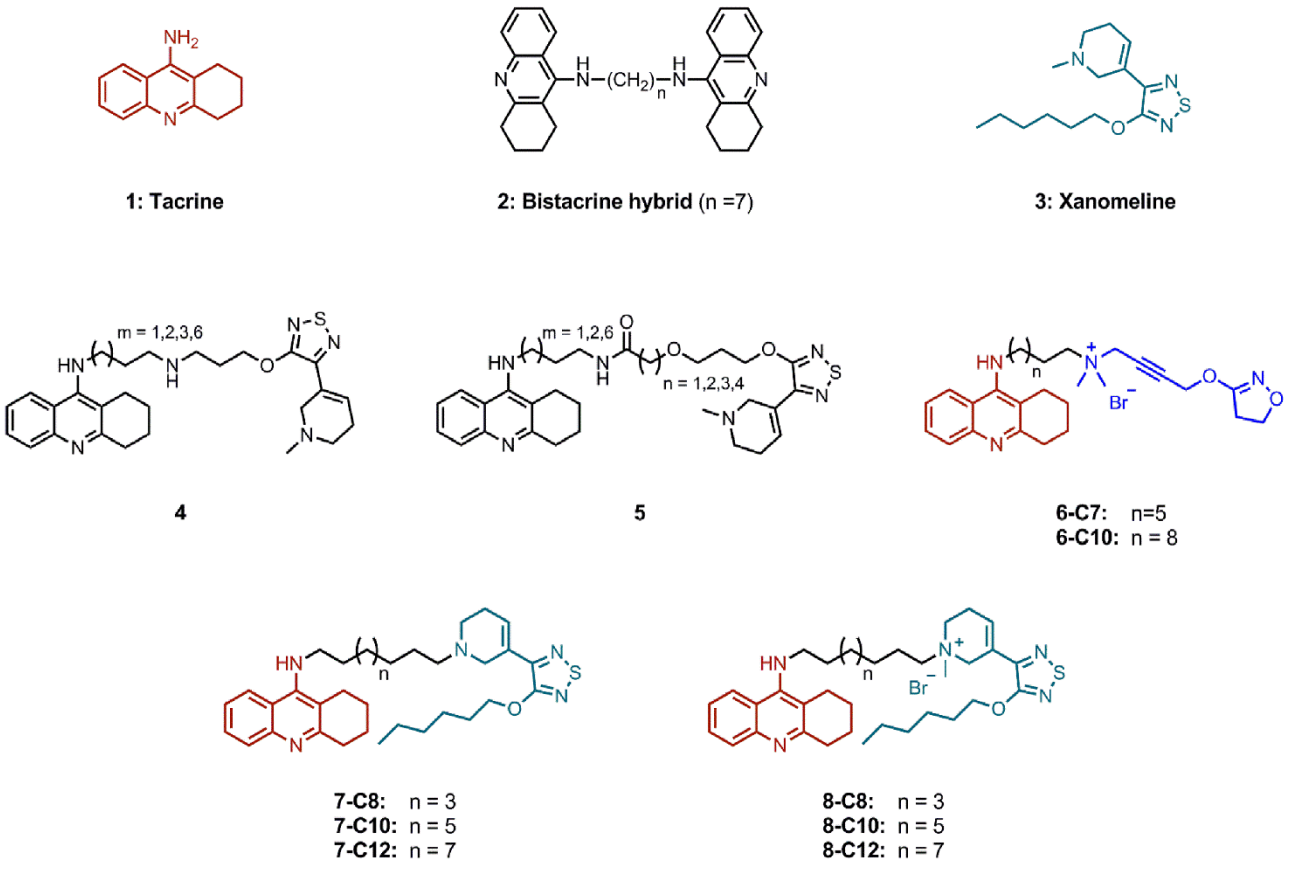


**Fig. 1.** Structures of reference compounds and of the known (**6-C7** and **6-C10**) and new (**7-C8**, **7-C10**, **7C12**, **8-C8**, **8-C10**, **8-C12**) tacrine-containing hybrid derivatives investigated in this study.

## 2. Results and discussion

### *2.1. Chemistry*

Tacrine **1** was synthesized following the literature procedure reported in Scheme 1 [31], which exploits the reaction of cyclohexanone with 2-aminobenzonitrile in the absence of solvent under zinc chloride catalysis. To import an alkyl linker chain at the amine function, **1** was reacted, in the presence of potassium hydroxide, with a large excess of commercially available dibromide derivatives of the respective spacer length, thus providing intermediate bromides **9a**, **9b** [32] and **9c**.

The orthosteric pharmacophoric moiety xanomeline was prepared following a Strecker-like known procedure [33], as reported in Scheme 1.

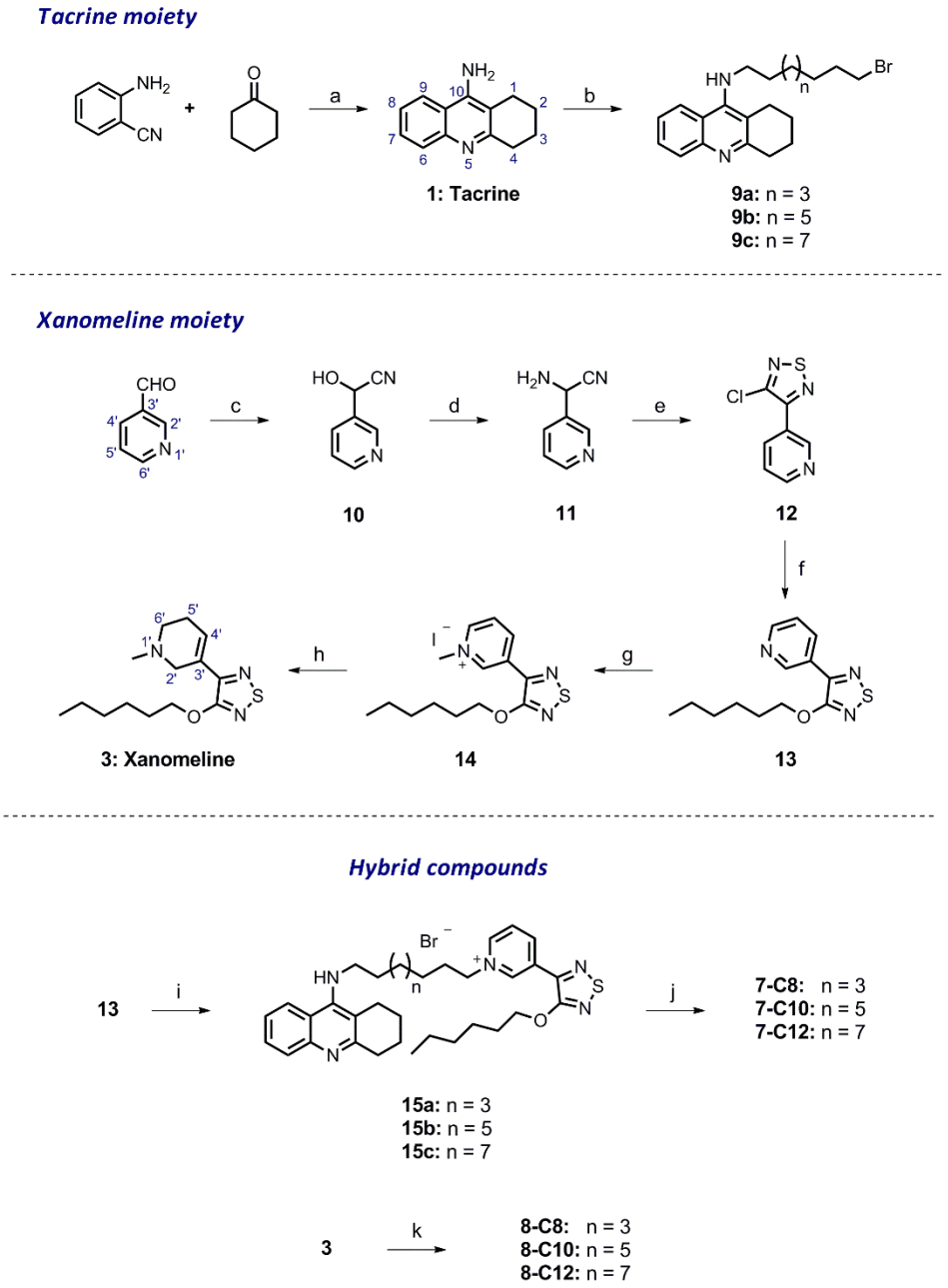


**Scheme 1.** Synthesis of target compounds. Reagents and conditions: (a) $ZnCl_2$, 120°C, 16 h; (b) $Br(CH_2)_nBr$ (n = 8 or 10 or 12), KOH, $CH_3CN$, 40°C, 72 h; (c) TMSCN, AcOH, r.t., 23 h; (d) $NH_3/NH_4Cl$, r.t., 22 h; (e) $S_2Cl_2$, DMF, 0 °C, 30 min; (f) 1-hexanol, NaH, THF, reflux, 3 h; (g) $CH_3I$, acetone, r.t., 22h; (h) $NaBH_4$, MeOH, r.t., 24 h; (i) **9a** (or **9b** or **9c**), DMF, 100 °C, 36 h; (j) $NaBH_4$, MeOH, r.t., 5 h. (k) **9a** (or **9b** or **9c**), $CH_3CN$, MW, 80 °C, 19 atm, 500 W, 10 h.

Briefly, the cyanohydrin **10** was obtained by treating commercially available 3-pyridinecarboxaldehyde with trimethylsilyl cyanide in the presence of acetic acid. Intermediate **10** was then converted into the corresponding aminonitrile derivative **11** by treatment with ammonium chloride in ammonium hydroxide. This intermediate was cyclized by reaction with disulfur dichloride

in *N*,*N*-dimethylformamide to give thiadiazole **12**, which, after nucleophilic substitution with 1-hexanol in the presence of sodium hydride, produced the functionalized thiadiazole **13**. The latter was reacted with methyl iodide in acetone to afford the corresponding quaternary ammonium salt **14**, which underwent reduction with sodium borohydride in methanol to the related tetrahydropyridinium moiety characterizing xanomeline **3**. Synthesis of the pyridine quaternary ammonium salts **15a-c** (Scheme 1) was performed by condensation of thiadiazole **13** with the respective tacrine-containing bromides **9a-c**; subsequent reduction of the pyridinium ring of intermediates **15a-c** with sodium borohydride afforded the desired hybrid compounds **7-Cn** (**7-C8**, **7C-10** and **7-C12**). Similarly, reaction of xanomeline **3** with bromides **9a-c** under microwave irradiation provided the permanently charged methylated analogs **8-Cn** (**8-C8**, **8C-10** and **8-C12**).

### *2.2. Biological activity and molecular modeling investigations*

#### *2.2.1. Acetylcholinesterase inhibitory activity*

The two groups of tacrine-xanomeline analogs **7-Cn** and **8-Cn** were tested for AChE inhibition by using the Ellman's test [34], and the resulting $pIC_{50}$ values were compared with those available for hybrids **6-Cn** (Table 1). We used the AChE from electric eel which, in our hands, gave quite comparable results to those obtained on related hybrids with the recombinant hAChE expressed in HEK 293 cells [3,27]. Both sets of compounds **7-Cn** and **8-Cn** were able to inhibit AChE; the tertiary amines **7-Cn** exhibited anticholinesterase activity ($pIC_{50}$ between 6.95 and 7.83) comparable to that of the model compound tacrine ($pIC_{50}$ = 7.73). Conversely, the quaternary tetrahydropiridinium derivatives **8-Cn** were more active ($pIC_{50}$ values between 8.12 and 9.55) than tacrine, with inhibitory potencies in the range of those shown by the tacrine-iperoxo hybrids **6-C7** ($pIC_{50}$ = 8.76) and **6-C10** ($pIC_{50}$ = 9.81).

**Table 1.** Cholinesterase activity of Tacrine and related hybrid compounds determined through the Ellman's test.

| Entry | AChE[a] $pIC_{50}$[b] [M] |
|---|---|
| **Tacrine** | 7.73 ± 0.04 |
| **7-C8** | 7.60 ± 0.12 |
| **7-C10** | 7.83 ± 0.06 |
| **7-C12** | 6.95 ± 0.13 |
| **8-C8** | 9.55 ± 0.12 |
| **8-C10** | 9.08 ± 0.06 |
| **8-C12** | 8.12 ± 0.08 |
| **6-C7** | 8.76 [27] |
| **6-C12** | 9.81 [27] |

[a]Experiments were performed in triplicate at AChE from electric eel (E.C. 3.1.1.7). [b]$pIC_{50}$ values are the negative logarithm of the concentration causing half-maximal inhibition of cholinesterase activity. Data are expressed as the mean ± S.E.M.

As far as the length of the spacer is taken into account, eight methylene units were optimal to impart the highest AChE inhibitory activity to the positively charged compounds (**8-C8**: $pIC_{50}$ = 9.55). For both series of tacrine-xanomeline derivatives, the longest chain compounds, with twelve methylene units, were those with the lowest inhibitory potency ($pIC_{50}$ = 6.95 for **7-C12** and $pIC_{50}$ = 8.12 for **8-C12**). On the other hand, comparison of the data evidenced in both **7-Cn** and **6-Cn** sets an inhibition peak with a spacer of ten methylene units ($pIC_{50}$ = 7.83 for **7-C10** and $pIC_{50}$ = 9.81 for **6-C10**), thus emphasizing a good tolerability of the linker length in the enzyme gorge between CAS and PAS.

### *2.2.2. Functional activity at $M_1$ mAChRs*

We studied the functional activity of all the compounds at the $M_1$ mAChR. Hence, we chose to investigate $M_1$AChR-mediated PLC response (see Split Luciferase Bioluminescence Assay) and inositol phosphate accumulation (see IP1 Accumulation Assay). Binding of ACh to mAChRs causes a conformational change in the receptor that promotes its association with an intracellular G protein determining its activation through the conversion of GTP to GDP on the G protein α subunit. The activated G protein dissociates from the receptor, acting as an enzyme to catalyze downstream intracellular events. The functional activity is mediated mainly by the physiologically relevant Gq-signaling pathway. Proteins of the $G\alpha_q$ family trigger the effector proteins phospholipases Cβ1-3 (PLCβ), leading to the hydrolysis of phosphatidylinositol 4,5-bisphosphate ($PIP_2$) to 1,2-diacylglycerol (DAG) and inositol-1,4,5-trisphosphate ($IP_3$). $IP_3$ mediates the release of $Ca^{2+}$ from intracellular compartments, notably from the endoplasmic reticulum.

### *2.2.3. Split Luciferase bioluminescence assay*

Littmann et al. [35] developed a split luciferase complementation assay to study the interaction of $M_1$ mAChR G protein with Phospholipase C, by expression of the newly $G\alpha_q$-PLC-β3 sensor in combination with $hM_1R$. With this assay, we assessed the early activation stage of interaction between the $G\alpha_q$ and phospholipase C-β3 for the new hybrids. Gα and PLC-β3 were fused on a DNA level with the split luciferase, in order to measure their interaction in terms of bioluminescence. The assay revealed the absence of receptor activation for the tacrine-xanomeline hybrids **7-Cn** and **8-Cn**. Regardless of the presence/absence of a quaternary ammonium head or the length of the spacer chain, these compounds did not show agonism at the $M_1$ mAChR since no activation of the phospholipase C was observed (Fig. 2A and 2B). Therefore, we may assume that these hybrids are unable to adopt a dualsteric binding mode, which triggers the activating functional response at the studied receptor. These findings are in line with those of Fang et al. [5], since also those tacrine-xanomeline hybrids (compounds **4** and **5**, Fig. 1) were found to prefer a purely allosteric binding mode [26,36], which

generates an inactive ligand-receptor complex at the $M_1$ subtype. On the contrary, the tacrine-iperoxo hybrids **6-C7** and **6-C10**, which already showed affinity for the $M_1$ mAChR in radioligand binding studies [27], activated the heterodimeric G protein (Fig. 2C), with $pEC_{50}$ values of 8.24 and 8.06, respectively (Table 2). These iperoxo-containing hybrids are indeed the most potent AChE inhibitors in the series with the additional ability to bind $M_1$ as well as $M_2$ mAChR subtypes.

**Table 2.** Maximal agonist effect and potency of hybrid compounds stimulating Gα and PLC-β3 interaction in CHO human $M_1$ cells.

| | Split-Luc assay | | |
|---|---|---|---|
| Entry | $E_{max}$[a] | $pEC_{50}$[b] | n |
| **6-C7** | 85.57 ± 1.50 | 8.24 ± 0.05 | 4 |
| **6-C10** | 78.14 ± 1.45 | 8.06 ± 0.05 | 4 |
| **7-C8** | n.a.[c] | n.a. | 3 |
| **7-C10** | n.a. | n.a. | 3 |
| **7-C12** | n.a. | n.a. | 3. |
| **8-C8** | n.a. | n.a. | 3 |
| **8-C10** | n.a. | n.a. | 3 |
| **8-C12** | n.a. | n.a. | 3 |
| **Xanomeline** | 100.70 ± 2.16 | 8.00 ± 0.07 | 3 |
| **Iperoxo** | 104.60 ± 0.85 | 8.89 ± 0.04 | 4 |
| **CCh** | 97.78 ± 1.71 | 6.25 ± 0.04 | 5 |
| **ACh** | 96.91 ± 1.28 | 6.88 ± 0.02 | 9 |
| | | $pIC_{50}$ | |
| **Atropine** | - | 10.06 ± 0.09 | 4 |

[a]$E_{max}$ is the maximal effect expressed as percentage. [b]$pEC_{50}$ is the concentration of the indicated compound inducing a half-maximal $G\alpha_q$-PLC activation. Data are normalized to the maximum response of the agonist carbachol. Data are expressed as the mean ± S.E.M. of three to nine independent experiments performed in triplicate. [c]n.a.: not applicable.

In terms of functional behavior, at the $M_1$ receptor derivatives **6-C7** and **6-C10** showed potency values comparable to those of iperoxo and xanomeline and even higher than those of carbachol and the endogenous agonist ACh. The measured efficacy values normalized to the carbachol (CCh)

reference ($E_{max}$ = 85.57% for **6-C7** and $E_{max}$ = 78.14% for **6-C10**) were instead lower than those of reference agonists (Fig. 2D and Table 2), thus engendering hybrid derivatives with a partial agonist profile. According to a model illustrated for bipharmacophoric partial agonists of $M_2$ mAChRs [36], **6-C7** and **6-C10** behave as "dynamic ligands", i.e. compounds that may bind to a receptor population in two distinct orientations, the dualsteric binding pose, inducing activation, and the purely allosteric binding pose that precludes receptor activation.

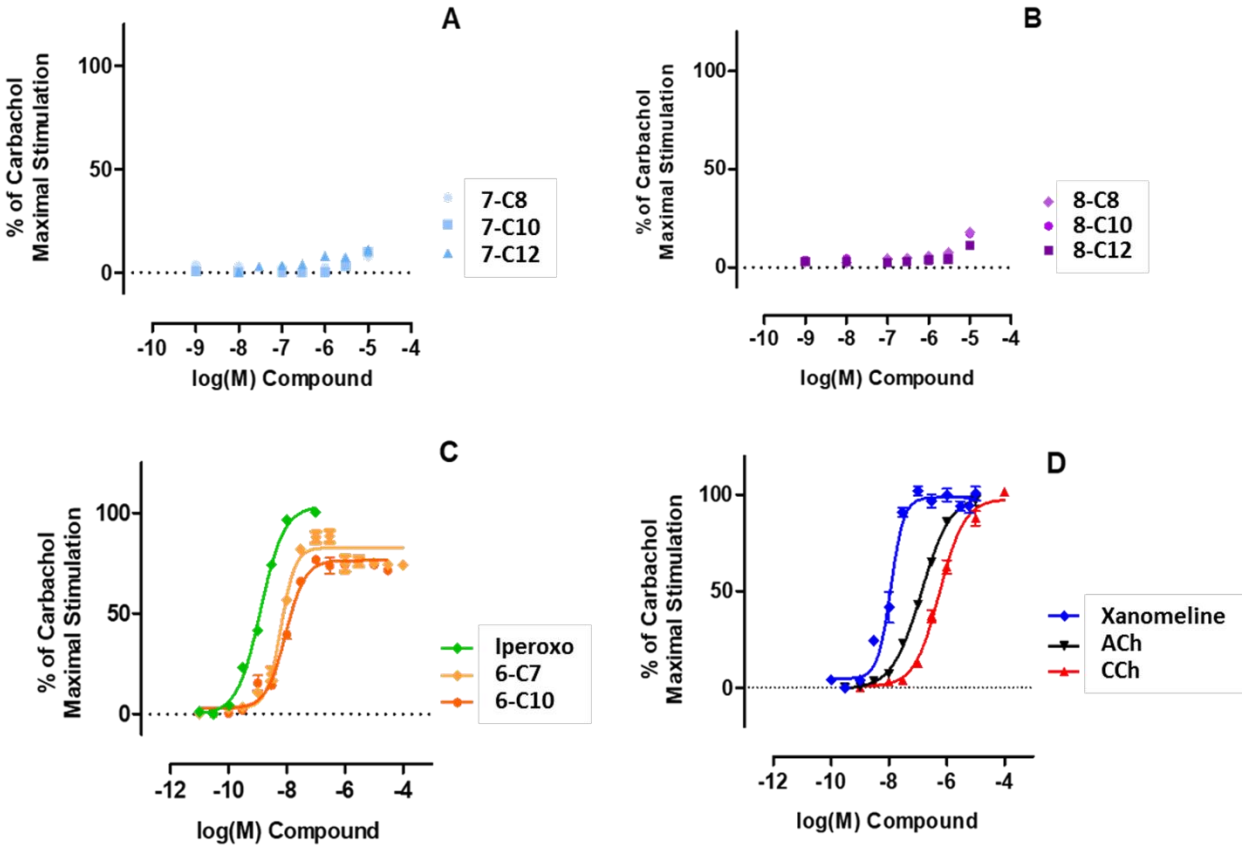


**Fig. 2.** Dose response curves obtained with the split luciferase assay.

Compounds **7-Cn** and **8-Cn** did not stabilize a G protein active conformation of the $M_1$ receptor and did not induce receptor stimulation when studied in the agonist mode (Fig. 2A and 2B); therefore, we evaluated their putative antagonist profile, by assessing the ability to counteract the effect of CCh at a concentration corresponding to $EC_{80}$ (3 μM). As illustrated in Fig. 3A and 3B, none of the six

structural analogs was able to compete with the agonist to reduce the degree of $G\alpha_q$-PLC activation. Conversely, as expected, the orthosteric antagonist atropine (blue curve) potently competed with CCh, with a $pIC_{50}$ value of 10.06 ± 0.09.

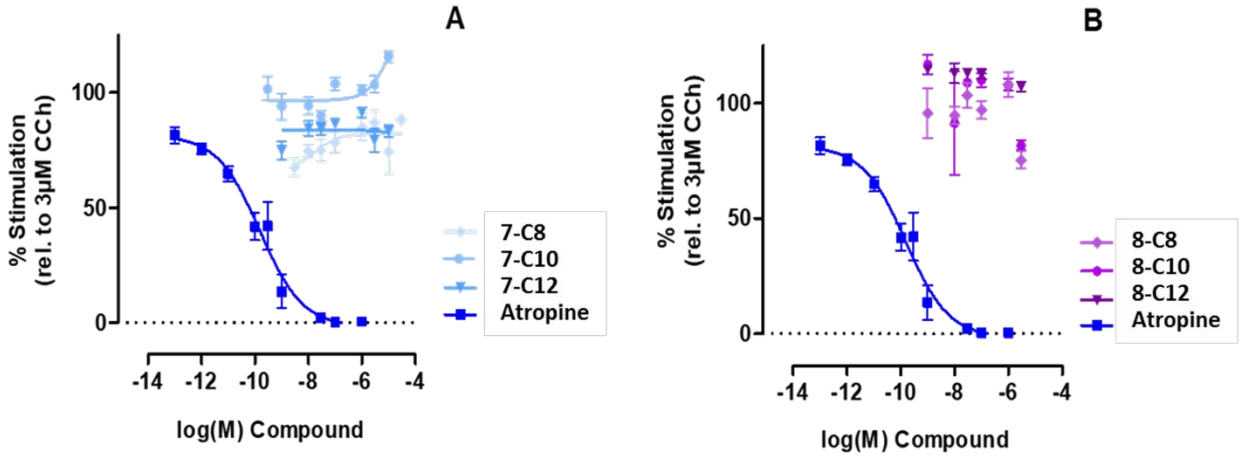


**Fig. 3.** Dose response curve of Split-Luc assay. Compounds **7-Cn** and **8-Cn** were measured in the antagonist mode. Data represent the mean ± S.E.M. of at least three independent experiments performed in triplicate.

Of note, compounds **7-Cn** and **8-Cn** did not cause cell death, since, despite their application up to 10 μM concentrations, $hM_1$ cells maintained the maximal response to G protein activation by 3 μM CCh. Therefore, in this cell line, these bipharmacophoric derivatives functionalized on the primary amine of tacrine with chains of different lengths linking orthosteric moieties (xanomeline as well as iperoxo), showed a marked reduction of toxicity with respect to tacrine. This behavior parallels the results we previously reported [3], since the toxicity of the **6-C10** bifunctional compound was also tested in HepG2 cells and found to be very low ($IC_{50}$: 32.2 ± 0.41 μM), making it an interesting outcome in view of developing putative drug candidates.

### *2.2.4. IP1 accumulation assay*

The measurement of $M_1R$-stimulated activation of the G protein-mediated pathway was performed applying the IP-One HTRF® assay (Cisbio, Codolet, France), which quantifies the accumulation of inositol phosphate, the degradation product of the second messenger inositol

triphosphate (IP3), through FRET-based experiments. The results obtained with the reference compounds and the hybrids **7-Cn** and **8-Cn** in the HTRF-IP1 assay are reported in Fig. 4. Xanomeline and ACh showed their ability to activate the downstream signaling response at the $M_1$ receptor, with $pIC_{50}$ values of 6.65 and 6.66, respectively (Fig. 4 and 5A), an outcome matching the second messenger assays reported in the literature [19,37-39]. By contrast, the allosteric fragment tacrine alone is unable to generate IP1 accumulation (Fig. 4).

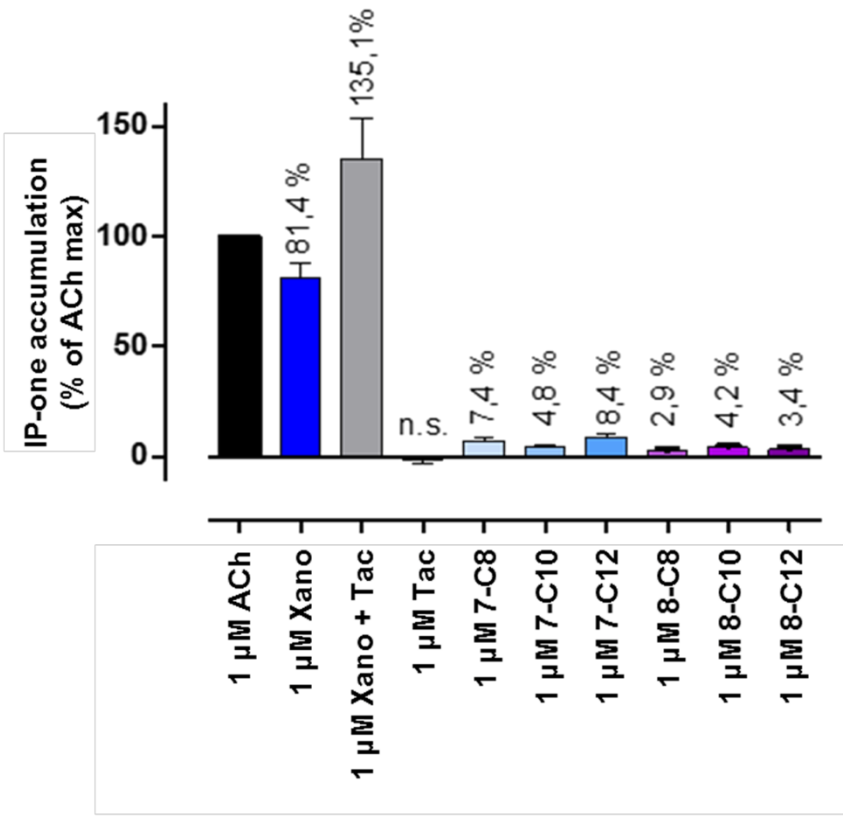


**Fig. 4.** Absence of IP1-accumulation by xanomeline (Xano)-tacrine (Tac) hybrids in live CHO-hM1 cells. Graph bars represent the mean ± S.E.M of three independent experiments performed in triplicate. Data not significantly different with ANOVA Tukey's Multiple Comparison Test ($P < 0.05$). n.s.: not significantly different from zero (one sample t test) ($P < 0.05$).

The application of a 1 µM tacrine and xanomeline combination resulted in a receptor activation response higher than that measured for xanomeline alone, which is indicative of the positive modulatory effect of tacrine at $M_1$ mAChRs. Conversely, the covalently bound tacrine-xanomeline molecular fragments were devoid of agonist activity in both sets of target hybrids **7-Cn** and **8-Cn** (Fig. 4), due to the lack of ligand-receptor interaction at the orthosteric recognition site and the

consequent inability to cause receptor activation. We extended the IP1 accumulation assay also to the tacrine-iperoxo hybrids **6-C7** and **6-C10** and obtained a very similar qualitative readout, in accordance with preliminary functional data [27]. After incubation with test compounds for 30 min at 37 °C, addition of detection reagents revealed the partial agonist profile of both dualsteric hybrids, with $pIC_{50}$ values of 7.05 and 6.90 for **6-C7** and **6-C10**, respectively (Table 3, Fig. 5B). Thus, in this second messenger IP1 assay, the partial agonism characterizing the two ligands ($E_{max}$ = 59.0 for **6-C7** and $E_{max}$ = 43.9 for **6-C10**, Table 3) became more evident than in the previous bioluminescence test.

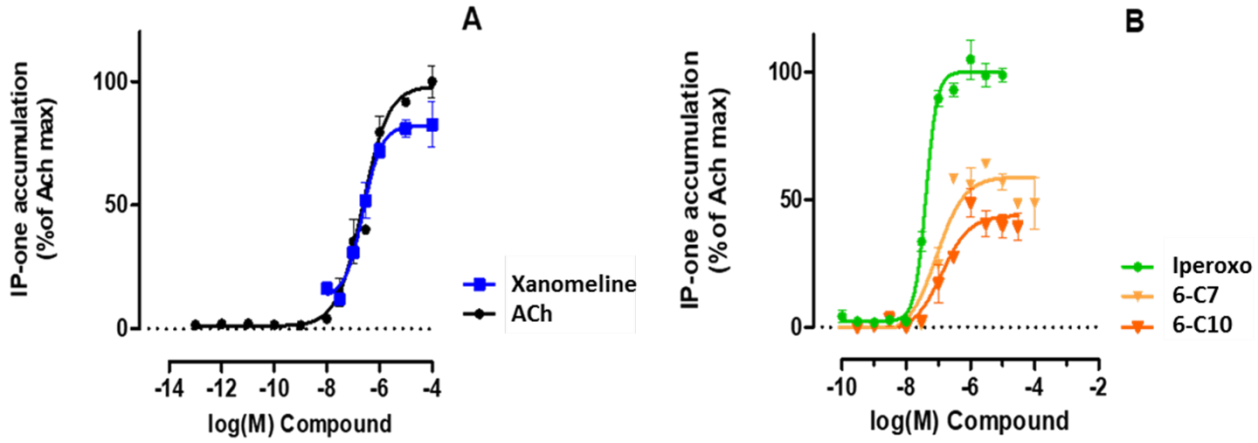


**Fig. 5.** Partial agonism for IP1 accumulation by hybrids **6-C7** and **6-C10** in live CHO-hM1 cells. Cells were treated with increasing concentrations of the indicated compounds for 30 min, and the resulting increase in intracellular inositol phosphates was measured as described in Materials and Methods. Curves drawn through the data points represent the best fit to the operational model of agonism. Data points are the mean ± S.E.M of three to five independent experiments performed in triplicate.

**Table 3.** Pharmacological parameters characterizing the effects of the indicated compounds on IP1-accumulation in live CHO-hM1 cells.

| | IP1 assay | | |
|---|---|---|---|
| Entry | $E_{max}$[a] | $pEC_{50}$[b] | n |
| **6-C7** | 59.00 ± 2.34 | 7.05 ± 0.11 | 4 |
| **6-C10** | 43.91 ± 2.80 | 6.90 ± 0.17 | 4 |
| **Iperoxo** | 102.50 ± 2.07 | 8.71 ± 0.07 | 4 |
| **Xanomeline** | 83.39 ± 3.34 | 6.65 ± 0.14[c] | 3 |
| **ACh** | 96.73 ± 3.10 | 6.66 ± 0.09[d] | 3 |

[a]$E_{max}$ is the maximal effect expressed as percentage of ACh (100 μM) effect. [b]$pEC_{50}$ is the concentration of the indicated compound inducing a half-maximal IP1 activation. Data are the mean ± S.E.M. of three or four independent experiments performed in triplicate. [c]Literature values: 6.08 [40], 6.96 [39]. [d]Literature values: 5.79 [39], 7.24 [37], 7.25 [41], 7.41 [40].

*2.2.5. Docking of Tacrine-Xanomeline hybrid compounds to AChE*

Computational docking studies were carried out to determine putative binding modes of the tacrine-xanomeline hybrid series **7-Cn** and **8-Cn**. Building on crystal structures of bis-tacrine derivatives [42] and previous docking calculations for other tacrine hybrids [3], a conserved binding mode of the tacrine moiety was assumed and a scaffold match constraint was applied to ensure its proper placement in the CAS, thereby reducing the search space and improving the convergence of the docking runs. For all hybrids, the constraint was readily satisfied in all docking calculations, leading to unstrained and well-scored binding poses in which the tacrine moiety adopts the standard orientation in the CAS (i.e., sandwiched between Trp84 and Phe330 and further stabilized by hydrogen bonding to His440, as known from crystal structures) and the linker protrudes into the AChE binding gorge.

The best representative poses of the methylammonium hybrids **8-Cn** show that the xanomeline moiety can be favorably placed in the PAS, yet with differences depending on the linker length (Fig. 6). For **8-C8**, the 1,2,5-thiadiazole ring is sandwiched between Tyr70 and Trp279 at ring-center distances of 4.0 and 3.7 Å, respectively (Fig. 6A). The tetrahydropyridine moiety remains in close contact (< 4 Å) with the indole ring of Trp279, whereas the hexyl chain spans the cavity between Tyr70 and Ile275. In the case of **8-C10**, the thiadiazole is also stacked between Tyr70 and Trp279 (with distances of 3.7 and 3.6 Å, respectively) (Fig. 6A). This, however, occurs in a slightly tilted orientation in which the thiadiazole ring is inverted with respect to **8-C8**, leading to a different orientation of the hexyl chain (directed back towards the gorge). This is a consequence of the extended linker and results in less favorable scores in comparison to **8-C8**. For **8-C12**, a similar binding mode as for **8-C10** can be identified among the docking results; however, this is found less frequently and scored much poorer by DSX than the binding pose shown in Fig. 6C. In the latter, the linker adopts a relaxed, extended conformation and the xanomeline moiety is no longer sandwiched in the PAS but interacts through weak polar contacts with Tyr70. Nevertheless, the scores do not reach the values

obtained by **8-C8**. As a consequence, the absolute values of both the DSX- and ASP-per-atom-scores of the **8-Cn** hybrids decrease in the order **8-C8** > **8-C10** > **8-C12**, in line with the ranking based on the experimental $pIC_{50}$ values.

The binding modes obtained for the **7-Cn** derivatives are very similar to those of the corresponding analogues **8-Cn** and are hence not discussed in detail here. The difference in inhibition potency between the **7-Cn** and **8-Cn** analogs can be rationalized on the basis of a higher desolvation cost for the tertiary nitrogen (in **7-Cn**) compared to the quaternary ammonium (in **8-Cn**), in analogy to other examples discussing the effect of amine methylation on binding affinity [43].

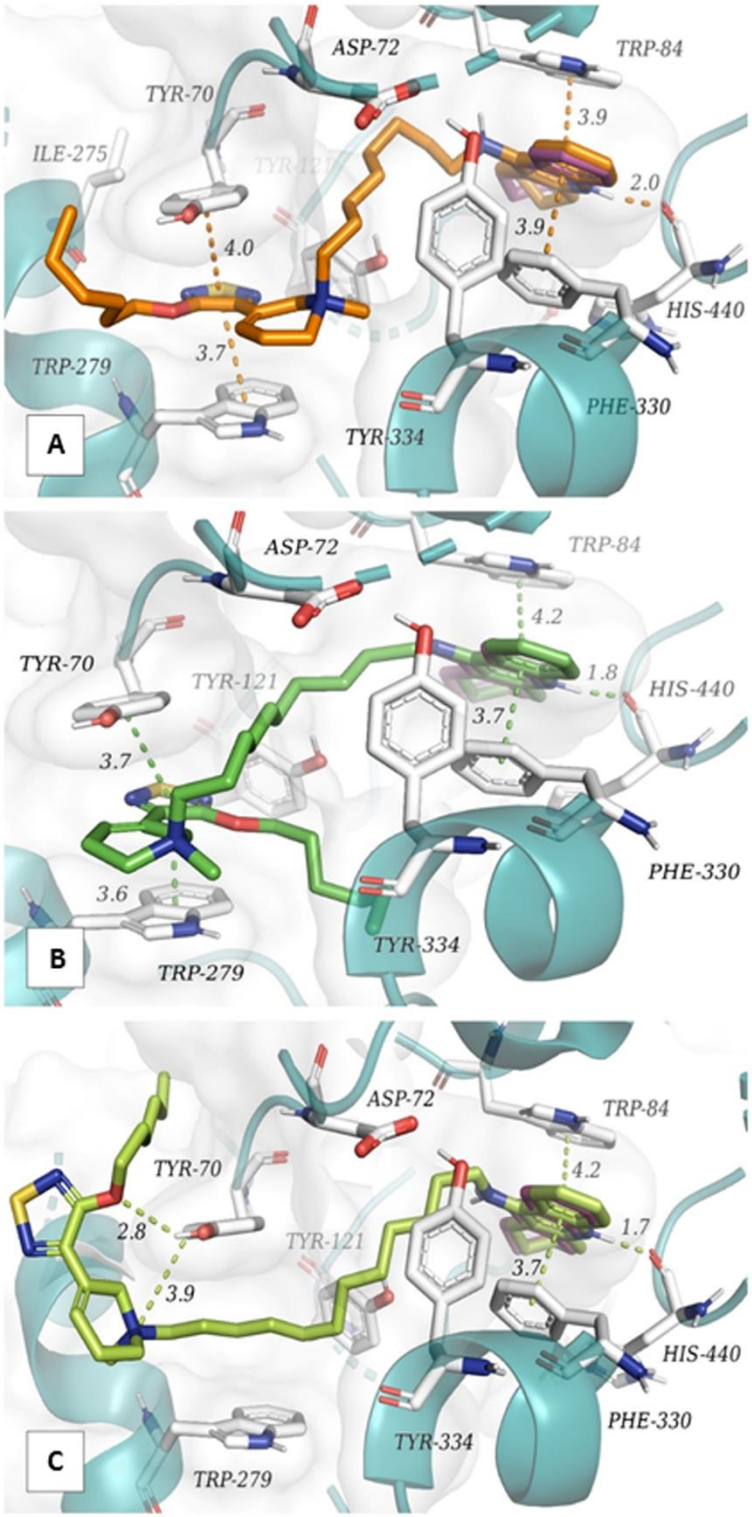


**Fig. 6.** Representative docking solutions for the methylammonium xanomeline-tacrine hybrids **8-C8** (A), **8-C10** (B) and **8-C12** (C). The binding poses illustrate the placement of the tacrine moiety in the CAS (with the tacrine scaffold match constraint depicted with magenta sticks), the linker chain in the gorge and the xanomeline part in or near the PAS. Most relevant contacts are highlighted and labeled with the corresponding distance (measured in Å).

## 3. Conclusions

In this study, we aimed at combining the multitarget with the bitopic ligand approaches through the synthesis of new hybrid ligands targeting both AChE and the $M_1$ mAChR subtype. The newly designed tacrine-xanomeline hybrids inhibited AChE with potency values higher than (**8-Cn**) or comparable to (**7-Cn**) that measured for the model compound tacrine. We found that the extent of anticholinesterase activity is affected by both, the permanently charged ammonium head and the length of the polymethylene spacer, derivative **8-C8** being the most potent inhibitor in the set of studied compounds. Docking calculations suggested a binding mode in which the tacrine moiety is placed in the catalytic active site, whereas the xanomeline moiety occupies the peripheral recognition pocket. This occurs most favorably with the C8 linker and least favorably with the C12 linker, in line with the observed activity profile.

In addition to their AChE inhibitory activity, the novel derivatives were assayed for $M_1$ mAChR agonism, the additional property we were searching for in their biological profile. However, hybrids **7-Cn** and **8-Cn** were unable to activate the $M_1$ receptor subtype, indicating that the response-activating dualsteric binding mode does not occur in this instance. We performed a parallel analysis on the two selected tacrine-iperoxo hybrids **6-C7** and **6-C10**, previously characterized by us for their relevant subnanomolar $IC_{50}$ values towards cholinesterases and their ability to bind $M_1$ and $M_2$ mAChRs. In this instance, the presence of the superagonist iperoxo as the orthosteric molecular fragment dictated G protein activation and IP1 accumulation, characterizing these two hybrid compounds as partial agonists at the $M_1$ receptor subtype. On the other hand, the xanomeline moiety, probably due to its hairpin structure, is not able to gain access to the orthosteric site, thus preventing activation of the $M_1$ receptor by hybrids **7-Cn** and **8-Cn**. Overall, comparable results were reported for the related hybrids **4** and **5**, bearing the same pharmacophoric elements (tacrine and xanomeline) with a different structural connection as well as different linker moieties.

Consistent with our data on $M_2$ mAChRs, the dualsteric binding mode of iperoxo-containing hybrid ligands also at the $M_1$ receptor is a useful starting point in view of further investigations. Moreover, **6-C7** and **6-C10**, despite their permanently charged nitrogen, showed an overall lipophilicity (log*P* equal to 2.05 and 3.28, respectively) [3], which is an indication of their propensity to act at the CNS. Taken together, these preliminary results suggest that a dual mechanism of action, i.e., combining AChE inhibition with activation of $M_1$ receptors in a single molecular entity, may represent a promising approach for a putative therapeutic intervention on a multifactorial pathology like Alzheimer's disease.

## 4. Materials and methods

### *4.1. Chemistry*

All chemicals were purchased from Sigma-Aldrich Srl (Milan, Italy and Schnelldorf, Germany), VWR (Darmstadt, Germany) and TCI (Eschborn, Germany) and were used without further purification. For chromatographic applications (HPLC, LC-MS), deionized water produced by means of a Milli-Q® system (Merck, Darmstadt, Germany) was used. HPLC grade and LC-MS grade solvents were from Sigma-Aldrich (Munich, Germany). The synthesis of some intermediates required inert atmosphere of argon or nitrogen and anhydrous conditions. The reactions was monitored by thin-layer chromatography (TLC) on commercial aluminum plates precoated with silica gel 60 (F-254, Merck) or with aluminum oxide (F-254, Fluka). Visualization was performed with UV light at 254 nm. Spots were further evidenced by spraying with a dilute alkaline potassium permanganate solution or an ethanol solution of phosphomolybdic acid and, for tertiary amines, with the Dragendorff reagent. The synthesized compounds were purified on glass chromatography columns packed with silica gel (230–400 mesh particle size, pore size 60 Å, Merck) or by flash chromatography on a puriFlash®430 system (Interchim, Montlucon, France) employing prepacked columns (Interchim, Montluçon, France) with silica gel filling (particle size 30 μm or 50 μm) for

normal-phase purifications; eluents have been specified from time to time. The detection was carried out by means of an UV detector and an Evaporative Light Scattering Detector (ELSD). Microwave assisted reactions were accomplished by means of a synthWAVE instrument (Milestone, Leutkirch, Germany). $^{1}$H NMR and $^{13}$C NMR spectra have been registered with a Bruker Avance 400 instrument (400 MHz and 100 MHz, respectively) or a Varian Mercury 300 instrument (300 MHz and 75 MHz, respectively). Chemical shifts ($\delta$) are expressed in parts-per-million (ppm) and coupling constants ($J$) in hertz (Hz). Abbreviations used for peak multiplicities are given as follows: s (singlet), bs (broad singlet), d (doublet), dd (doublet of doublets), ddd (doublet of doublet of doublets), dddd (doublet of doublet of doublet of doublets), t (triplet), q (quartet), quint (quintet), m (multiplet). Melting points have been determined with a Büchi Mod. B 540 apparatus and are uncorrected. The HPLC and mass analyses were performed on a Shimadzu LCMS-2020 system equipped with a DGU-20A3R degassing unit, a LC20AB liquid chromatograph and a SPD-20A UV/Vis detector. A Synergi 4U fusion -RP (150 × 4.6 mm) column was used as stationary phase. A gradient mobile phase consisting of 0.1% formic acid in water (solvent A) and 0.1% formic acid in MeOH (solvent B) was used. The time program elution was as follows: solvent A from 0% to 90% in 13 min, then 90% for 5 min, from 90% to 5% in 1 min, then 5% for 4 min. The flow rate was 1.0 mL/min and UV detection was measured at 254 nm. All final compounds were found to have a ≥ 95% purity. Mass spectra were recorded in ESI-positive mode and the data are reported as mass-to-charge ratio (m/z) of the corresponding positively charged molecular ions. The tacrine-iperoxo hybrid derivatives **6-C7** and **6-C10** were prepared according to known procedures [3].

### *4.2. Preparation of Tacrine moiety: Synthesis of 1,2,3,4-tetrahydroacridin-9-amine (**1**)*

Zinc chloride (3.47 g, 25.4 mmol) was added to a mixture of 2-aminobenzonitrile (3 g, 25.4 mmol) and cyclohexanone (30.5 mL, 294.6 mmol). The reaction was kept at 120°C for 16 h, then cooled to room temperature and the solvent was evaporated under reduced pressure. To the residue,

50 mL of AcOEt were added and the resulting solid was collected after filtration. To the solid, 65 mL of a 10% solution of NaOH in water was poured and kept under stirring overnight. After filtration, the cake was washed with $H_2O$ (3 × 20 mL), and then kept under stirring overnight with 30 mL of MeOH. The solid was filtered and the solvent was evaporated under reduced pressure to give tacrine **1** as a yellow solid (4,95 g, 98%): $R_f$ = 0.47 ($CHCl_3$/MeOH/$NH_3$ 7:3:0,1). mp = 178–181 °C. $^1$H NMR (400 MHz, $CDCl_3$): $\delta$ 7.89 (dd, $J$ = 8.5, 0.6 Hz, 1H; H9), 7.68 (dd, $J$ = 8.4, 0.8 Hz, 1H; H6), 7.55 (ddd, $J$ = 8.4, 6.8, 1.3 Hz, 1H; H7), 7.35 (ddd, $J$ = 8.2, 6.8, 1.2 Hz, 1H; H8), 4.65 (s, $J$ = 42.8 Hz, 2H; $NH_2$), 3.01 (t, $J$ = 9.9 Hz, 2H; H4), 2.60 (t, $J$ = 6.2 Hz, 2H; H1), 1.99-1.84 (m, 4H; 2×H2, 2×H3). $^{13}$C NMR (101 MHz, $CD_3OD$): $\delta$ 158.45, 150.72, 146.73, 129.84, 127.25, 124.51, 122.32, 118.20, 110.50, 33.86, 24.53, 23.76, 23.71.

### *4.3. General procedure for the synthesis of intermediates **9a-c***

To a solution of tacrine (**1**) (1 equiv) in $CH_3CN$ (0.1 M) was added KOH (2 equiv) and the reaction was kept under stirring for 2 h. Then, a solution of the appropriate dibromoalkane (10 equiv) in $CH_3CN$ (4 M) was added. The reaction was kept for 3 days at 40 °C, then the mixture was purified through silica gel column chromatography, using DCM/MeOH 99:1 → 9:1 as eluent, thus providing intermediates **9a-c** as pure compounds.

#### *4.3.1. N-(8-Bromooctyl)-1,2,3,4-tetrahydroacridin-9-amine (**9a**)*

The title compound was prepared by reacting **1** (400 mg, 2.02 mmol), KOH (135 mg, 2.42 mmol) and 1,8-dibromooctane (5.48 g, 20.18 mmol) in $CH_3CN$ (25 mL). After standard workup, **9a** was obtained as a yellow oil (250 mg, 32%): $R_f$ = 0.50 (DCM/MeOH 9:1). $^1$H NMR (400 MHz, $CDCl_3$): $\delta$ 8.68 (d, $J$ = 8.5, 1H; H9), 8.18 (d, $J$ = 8.6 Hz, 1H; H6), 7.73 (m, 1H; H7), 7.47 (t, $J$ = 7.85 Hz, 1H; H8), 5.51 (s, 1H; NH), 3.94 (dd, $J$ = 12.3, 6.8 Hz, 2H; $CH_2$−Br), 3.40 (m, 4H; HN−C$H_2$, H4), 2.58 (t, $J$ = 5.9, 2H; H1), 1.92–1.83 (m, 8H; 2×H2, 2×H3, C$H_2$−$CH_2$−Br, HN−$CH_2$−C$H_2$), 1.48–1.38 (m, 8H; HN−$(CH_2)_2$−C$H_2$−C$H_2$−C$H_2$−C$H_2$−$(CH_2)_2$−Br). $^{13}$C NMR (101 MHz, $CDCl_3$): $\delta$ 155.41, 151.19,

139.29, 131.91, 124.89, 124.61, 120.76, 116.06, 111.41, 48.26, 34.06, 32.60, 3.91, 28.97, 28.81, 28.52, 27.91, 26.56, 24.25, 22.00, 20.82.

*4.3.2. N-(10-Bromodecyl)-1,2,3,4-tetrahydroacridin-9-amine (**9b**)*

The title compound was prepared by reacting **1** (450 mg, 2.27 mmol), KOH (255 mg, 4.54 mmol) and 1,10-dibromodecane (6.81 g, 22.70 mmol) in $CH_3CN$ (25 mL). After standard workup, **9b** was obtained as a yellow oil (308 mg , 35%): $R_f$ = 0,51 (DCM/MeOH 9:1). $^1$H NMR (400 MHz, $CDCl_3$): $\delta$ 7.94 (t, $J$ = 8.1 Hz, 2H; H9, H6), 7.50 (t, $J$ = 7.6 Hz, 1H; H7), 7.30 (t, $J$ = 7.6, 1H; H8), 4.28 (s, 1H; NH), 3.49 (t, $J$ = 7,1 Hz, 2H; $CH_2$−Br), 3.34 (td, $J$ = 6.8, 1.5 Hz, 2H; HN−C$H_2$), 3.04 (s, 2H; H4), 2.65 (s, 2H; H1), 1.92–1.83 (m, 4H; 2×H2, 2×H3), 1.83–1.74 (m, 2H; C$H_2$−$CH_2$−Br), 1.68–1.58 (m, 2H; HN−$CH_2$−C$H_2$), 1.44–1.13 (m, 12H; HN−$(CH_2)_2$−C$H_2$−C$H_2$−C$H_2$−C$H_2$−C$H_2$−C$H_2$−$(CH_2)_2$−Br). $^{13}$C NMR (101 MHz, $CDCl_3$). $\delta$ 155.11, 151.13, 139.41, 131.51, 124.58, 124.47, 120.72, 116.06, 111.49, 48.06, 33.94, 32.52, 30.75, 29.11, 29.05, 28.94, 28.84, 28.43, 27.85, 26.49, 24.21, 21.88, 20.74.

*4.3.3. N-(10-Bromododecyl)-1,2,3,4-tetrahydroacridin-9-amine (**9c**)*

The title compound was prepared by reacting **1** (250 mg, 1.26 mmol), KOH (141 mg, 2.52 mmol) and 1,12-dibromododecane (3.31 g, 10.09 mmol) in $CH_3CN$ (15 mL). After standard workup, **9c** was obtained as a yellow oil (250 mg , 51%): $R_f$ = 0,56 (DCM/MeOH 9:1). $^1$H NMR (400 MHz, $CDCl_3$): $\delta$ 8.32 (d, $J$ = 8.3, 1H; H9), 8.22 (d, $J$ = 8.7, 1H; H6), 7.54 (t, $J$ = 7.6, 1H; H7), 7.33 (t, $J$ = 7.7, 1H; H8), 3.87 (t, $J$ = 7.1 Hz, 2H; $CH_2$−Br), 3.29 (t, $J$ = 6.8 Hz, 2H; HN−C$H_2$), 3.19–3.06 (m, 2H; H4), 2.73–2.58 (m, 2H; H1), 1.88–1.59 (m, 8H; 2×H2, 2×H3, C$H_2$−$CH_2$−Br, HN−$CH_2$−C$H_2$), 1.39–0.96 (m, 16H; HN−$(CH_2)_2$−C$H_2$−C$H_2$−C$H_2$−C$H_2$−C$H_2$−C$H_2$−C$H_2$−$(CH_2)_2$−Br). $^{13}$C NMR (101 MHz, $CDCl_3$): $\delta$ 155.74, 150.46, 138.55, 132.03, 124.82, 124.74, 120.01, 115.68, 111.05, 103.13, 48.06, 45.11, 34.04, 32.68, 30.81, 29.35, 29.27, 29.11, 28.60, 28.31, 28.01, 26.62, 24.24, 21.88, 20.62.

*4.4. Preparation of Xanomeline moiety: Synthesis of 2-hydroxy-2-(pyridin-3-yl)acetonitrile (**10**)*

A water solution of 3-pyridinecarboxaldheyde (3.00 g, 28.01 mmol) and acetic acid (28.01 mmol, 1.68 g) were added to a water solution of TMSCN (3.71 g, 37.21 mmol) at 0°C. The reaction proceeded at room temperature for 23 h and then was extracted with AcOEt (3 × 20 mL). The pooled organic phases were dried over anhydrous $Na_2SO_4$ and the solvent was evaporated under reduced pressure, giving the desired product **10** as a yellow-orange oil (3,36 g, 78%): $R_f$ = 0.44 (AcOEt). $^1$H NMR (300 MHz, $CDCl_3$): $\delta$ 8.62 (d, $J$ = 2.0 Hz, 1H; H2′), 8.53 (d, $J$ = 4.7 Hz, 1H; H6′), 7.96 (dt, $J$ = 7.9, 1.6 Hz, 1H; H4′), 7.42 (dd, $J$ = 7.9, 5.0 Hz, 1H; H5′), 5.65 (s, 1H; CH−CN). $^{13}$C NMR (75 MHz, $CDCl_3$): $\delta$ 149.70, 147.10, 135.58, 133.08, 124.50, 118.81, 61.05.

*4.4.1. 2-Amino-2-(pyridin-3-yl)acetonitrile (**11**)*

To a water solution of $NH_4Cl$ (7.93 g, 148.17 mmol), 4 mL of $NH_3$ (33% in water) and then a water solution of **10** (2.65 g, 19.76 mmol) were added dropwise. The reaction was kept at room temperature for 22 h. The aqueous phase was extracted four times with 10 mL of DCM, and four times with 10 mL of a mixture of DCM/*i*PrOH (7:3). The pooled organic phases were dried over anhydrous $Na_2SO_4$ and concentrated under reduced pressure, giving the desired product **11** as an orange oil (1.160 g, 44%): $R_f$ = 0.52 (DCM/MeOH 9:1). $^1$H NMR (300 MHz, $CDCl_3$): $\delta$ 8.80 (d, $J$ = 2.3 Hz, 1H; H2′), 8.64 (dd, $J$ = 4.8, 1.4 Hz, 1H; H6′), 7.89 (dt, $J$ = 8.0, 1.7 Hz, 1H; H4′), 7.36 (dd, $J$ = 8.0, 4.8 Hz, 1H; H5′), 4.97 (s, 1H; CH−CN), 2.00 (s, 2H; $NH_2$). $^{13}$C NMR (75 MHz, $CDCl_3$): $\delta$ 150.28, 148.24, 134.37, 132.09, 123.70, 120.02, 45.20.

*4.4.2. 3-Chloro-4-(pyridin-3-yl)-1,2,5-thiadiazole (**12**)*

A solution of **11** (1.15 g, 8.64 mmol) in 5 mL of DMF and $S_2Cl_2$ (1.38 mL, 17.27 mmol) was added dropwise to 10mL of DMF at 0°C. After 30 min, 20 mL of water were poured and the suspension was filtered. The filtrate was basified with 9M NaOH (10 mL), and the aqueous phase

was extracted with DCM (3 × 20 mL). The pooled organic phases were dried over anhydrous $Na_2SO4$, concentrated under reduced pressure, affording the desired product **12** as a brown solid (1.35 g, 79%): $R_f$ = 0.30 (cyclohexane/AcOEt 3:2). mp = 51–53 °C. $^1$H NMR (300 MHz, $CDCl_3$): $\delta$ 9.14 (d, $J$ = 2.1 Hz, 1H; H2′), 8.66 (dd, $J$ = 4.8, 1.5 Hz, 1H; H6′), 8.21 (dt, $J$ = 8.1, 1.7 Hz, 1H; H4′), 7.38 (dd, $J$ = 7.9, 4.8 Hz, 1H; H5′). $^{13}$C NMR (75 MHz, $CDCl_3$): $\delta$ 155.09, 150.83, 149.21, 143.44, 135.68, 126.82, 123.31.

*4.4.3. 3-(Hexyloxy)-4-(pyridin-3-yl)-1,2,5-thiadiazole (**13**)*

A suspension of 60% NaH (1,48 g, 61.47 mmol) in anhydrous THF (3mL) was added dropwise to a solution of 1-hexanol (2.09 g, 20.49 mmol) in anhydrous THF (6mL) at 0 °C. The suspension was kept under stirring at room temperature for 2 h. A solution of **12** (1.35 g, 6.83 mmol) in anhydrous THF (5mL) was added dropwise to the suspension. The reaction was kept under reflux for 3h and then quenched with 10 mL of a saturated aqueous solution of $NaHCO_3$. The aqueous phase was extracted with DCM (3 × 10 mL), the pooled organic phases were dried over anhydrous $Na_2SO_4$ and then concentrated under reduced pressure. The crude was purified through silica gel column chromatography, using as eluent cyclohexane/AcOEt 9:1. The desired product **13** was obtained as a white solid (1.53 g, 85%): $R_f$ = 0.41 (cyclohexane/AcOEt 4:1). mp = 49–51 °C. $^1$H NMR (300 MHz, $CDCl_3$): $\delta$ 9.41 (dd, $J$ = 2.2, 0.7 Hz, 1H; H2′), 8.66 (dd, $J$ = 4.8, 1.6 Hz, 1H; H6′), 8.46 (dt, $J$ = 8.1, 1.9 Hz, 1H; H4′), 7.42 (ddd, $J$ = 8.1, 4.9, 0.7 Hz, 1H; H5′), 4.53 (t, $J$ = 6.7 Hz, 2H; $CH_2$−O), 1.89 (quint, $J$ = 6.9 Hz, 2H; C$H_2$−$CH_2$−O), 1.67–0.89 (m, 6H; $CH_3$−C$H_2$−C$H_2$−C$H_2$−$(CH_2)_2$−O), 0.91 (t, $J$ = 5.6 Hz, 3H; C$H_3$−$(CH_2)_5$−O). $^{13}$C NMR (75 MHz, $CDCl_3$): $\delta$ 162.85, 150.12, 148.65, 144.95, 134.66, 127.67, 123.37, 71.45, 31.44, 28.88, 25.69, 22.54, 14.00.

*4.4.4. 1-Methyl-3-(4-(pentyloxy)-1,2,5-thiadiazol-3-yl)pyridin-1-ium iodide (**14**)*

Iodomethane (1.08 g, 7.59 mmol) was added dropwise to a solution of **13** (500 mg, 1.90 mmol) in 4 mL of acetone. The reaction proceeded for 26 h at room temperature, then the solution was

concentrated under reduced pressure, and washed with $Et_2O$ (10 mL). The desired product **14** was obtained as a yellow oil (733 mg, 95%): $R_f$ = 0.30 (DCM/MeOH 4:1). $^1$H NMR (300 MHz, $CDCl_3$): $\delta$ 9.60 (d, $J$ = 5.4 Hz, 1H; H2′), 9.45 (s, 1H; H6′), 9.11 (d, $J$ = 8.2 Hz, 1H; H4′), 8.28 (dd, $J$ = 8.3, 5.4 Hz, 1H; H5′), 4.79 (s, 3H; $CH_3{-}N^+$), 4.57 (t, $J$ = 6.9 Hz, 2H; $CH_2{-}O$), 1.91 (quint, $J$ = 6.9 Hz, 2H; $CH_2{-}CH_2{-}O$), 1.59–1.13 (m, 6H; $CH_3{-}CH_2{-}CH_2{-}CH_2{-}(CH_2)_2{-}O$), 0.88 (t, $J$ = 6.3 Hz, 3H; $CH_3{-}(CH_2)_5{-}O$). $^{13}$C NMR (75 MHz, $CDCl_3$): $\delta$ 163.13, 145.73, 142.86, 141.88, 139.45, 131.47, 128.65, 72.49, 50.67, 31.34, 28.72, 25.54, 22.52, 13.99.

*4.4.5. 3-(Hexyloxy)-4-(1-methyl-1,2,5,6-tetrahydropyridin-3-yl)-1,2,5-thiadiazole (**3**)*

A solution of $NaBH_4$ (273 mg, 7.20 mmol) in 3 mL of MeOH was added dropwise to a solution of **14** (730 mg, 1.80 mmol) in 5 mL of MeOH. The reaction was kept under stirring at room temperature for 2.5 days. After quenching with 10 mL of water, the aqueous phase was extracted with DCM (3 × 10 mL). The pooled organic phases were dried over anhydrous $Na_2SO_4$ and then concentrated under reduced pressure. The crude was purified through silica gel column chromatography, using as eluent DCM/MeOH 95:5. Xanomeline **3** was obtained as a yellow-orange oil (383 mg, 75%): $R_f$ = 0.30 (DCM/MeOH 95:5). $^1$H NMR (300 MHz, $CDCl_3$): $\delta$ 7.16–6.96 (m, 1H; H4′), 4.44 (t, $J$ = 6.6 Hz, 2H; $CH_2{-}O$), 3.51 (d, $J$ = 2.0 Hz, 2H; H2′), 2.63 (t, $J$ = 5.7 Hz, 2H; H6′), 2.50 (s, 5H; $CH_3{-}N$, 2×H5′), 1.83 (quint, $J$ = 6.9 Hz, 2H; $CH_2{-}CH_2{-}O$), 1.58–1.12 (m, 6H; $CH_3{-}CH_2{-}CH_2{-}CH_2{-}(CH_2)_2{-}O$), 0.90 (t, $J$ = 6.6 Hz, 3H; $CH_3{-}(CH_2)_5{-}O$). $^{13}$C NMR (75 MHz, $CDCl_3$): $\delta$ 162.49, 146.55, 128.86, 128.18, 70.93, 54.74, 51.08, 45.68, 31.34, 28.76, 26.28, 25.60, 22.48, 13.94.

*4.5. Preparation of Tacrine-Xanomeline hybrid compounds: General procedure for the synthesis of intermediates **15a-c***

A solution of compound **13** (1 equiv) in DMF (0.1 M) was added to a solution of functionalized tacrine-incorporating bromide (**9a-c**) (1 equiv) in DMF (0.1 M). The mixture was stirred in a sealed

reaction tube for 36 h at 100 °C. The crude reaction mixture was passed through a silica plug, eluting with DCM/MeOH 100:0 → 4:1. The isolated desired compound was used without any further purification.

*4.5.1. 3-(4-(Hexyloxy)-1,2,5-thiadiazol-3-yl)-1-(8-((1,2,3,4-tetrahydroacridin-9-yl)amino)octyl)pyridin-1-ium bromide (**15a**)*

The title compound was prepared by reacting **13** (300 mg, 1,14 mmol) and **9a** (443 mg, 1.14 mmol) in DMF (20 mL). After standard workup, **15a** was obtained as a yellow oil (159 mg , 21%): $R_f$ = 0.20 (DCM/MeOH 9:1). $^1$H NMR (400 MHz, $CD_3OD$): $\delta$ 9.61 (s, 1H; H2′), 9.23 (dt, $J$ = 8.3, 1.3 Hz, 1H; H4′), 9.10 (d, $J$ = 6.1 Hz, 1H; H6′), 8.39 (d, $J$ = 8.6 Hz, 1H; H5′), 8.26 (dd, $J$ = 8.2, 6.1 Hz, 1H; H9), 7.84 (ddd, $J$ = 6.8, 3.1, 1.5 Hz, 1H; H6), 7.79 (dd, $J$ = 8.5, 1.2 Hz, 1H; H7), 7.58 (ddd, $J$ = 7.1, 3.3, 1.5 Hz, 1H; H8), 4.77 (t, $J$ = 7.6 Hz, 2H; $CH_2$−$N^+$), 4.62 (t, $J$ = 6.7 Hz, 2H; $CH_2$−O), 3.95 (t, $J$ = 7.4 Hz, 2H; HN−C$H_2$), 3.03 (t, $J$ = 5.6 Hz, 2H; H4), 2.71 (t, $J$ = 5.4 Hz, 2H; H1), 2.09 (quint, $J$ = 7.2 Hz, 2H; C$H_2$−$CH_2$−O), 2.00–1.91 (m, 6H; C$H_2$−$CH_2$−$N^+$, 2×H2, 2×H3), 1.89–1.78 (m, 2H; HN−$CH_2$−C$H_2$), 1.54–1.28 (m, 14H; HN−$(CH_2)_2$−C$H_2$−C$H_2$−C$H_2$−C$H_2$−$(CH_2)_2$−$N^+$, $CH_3$−C$H_2$−C$H_2$−C$H_2$−$(CH_2)_2$−O), 0.91 (t, $J$ = 7.1 Hz, 3H; C$H_3$−$(CH_2)_5$−O). $^{13}$C NMR (101 MHz, $CD_3OD$): $\delta$ 164.47, 157.91, 151.70, 145.57, 144.21, 143.81, 141.87, 139.77, 134.04, 133.22, 129.67, 126.46, 126.31, 120.15, 117.03, 112.82, 73.32, 63.60, 49.10, 32.64, 32.45, 31.52, 30.08, 30.00, 29.85, 29.30, 27.63, 27.12, 26.74, 24.93, 23.62, 22.98, 21.83, 14.38.

*4.5.2. 3-(4-(Hexyloxy)-1,2,5-thiadiazol-3-yl)-1-(10-((1,2,3,4-tetrahydroacridin-9-yl)amino)decyl)pyridin-1-ium bromide (**15b**)*

The title compound was prepared by reacting **13** (250 mg, 0.949 mmol) and **9b** (396 mg, 0.949 mmol) in DMF (20 mL). After standard workup, **15b** was obtained as a yellow oil (148 mg, 23%): $R_f$ = 0.24 (DCM/MeOH 9:1). $^1$H NMR (400 MHz, $CDCl_3$): $\delta$ 10.36 (d, $J$ = 6.0 Hz, 1H; H2′), 9.38 (s, 1H; H4′), 9.07 (dd, $J$ = 9.7, 1.3 Hz, 1H; H6′), 8.25 (dd, $J$ = 8.2, 6.1 Hz, 1H; H5′), 7.94 (dd, $J$ = 23.1,

8.3 Hz, 2H; H9, H6), 7.51 (ddd, *J* = 8.3, 6.8, 1.3 Hz, 1H; H7), 7.31 (ddd, *J* = 8.2, 6.8, 1.2 Hz, 1H; H8), 5.14 (t, *J* = 7.5 Hz, 2H; $CH_2$−$N^+$), 4.57 (t, *J* = 6.8 Hz, 2H; $CH_2$−O), 3.55–3.42 (m, 2H; HN−C*H*$_2$), 3.05 (s, 2H; H4), 2.70 (s, 2H; H1), 2.06 (dd, *J* = 14.6, 7.5 Hz, 2H; C*H*$_2$−$CH_2$−O), 1.95–1.84 (m, 6H C*H*$_2$−$CH_2$−$N^+$, 2×H2, 2×H3), 1.63 (dd, *J* = 14.0, 7.1 Hz, 2H; HN−$CH_2$−C*H*$_2$), 1.51–1.09 (m, 18H; HN−$(CH_2)_2$−C*H*$_2$−C*H*$_2$−C*H*$_2$−C*H*$_2$−C*H*$_2$−C*H*$_2$−$(CH_2)_2$−$N^+$, $CH_3$−C*H*$_2$−C*H*$_2$−C*H*$_2$−$(CH_2)_2$−O), 0.89 (t, *J* = 7.1 Hz, 3H; C*H*$_3$−$(CH_2)_5$−O) $^{13}$C NMR (101 MHz, $CD_3OD$): *δ* 164.46, 157.91, 151.75, 145.57, 144.16, 143.84, 141.85, 139.82, 134.00, 133.23, 129.68, 126.41, 126.26, 120.22, 117.05, 112.81, 73.32, 63.63, 49.13, 32.64, 32.48, 31.55, 30.50, 30.41, 30.29, 30.13, 29.86, 29.28, 27.72, 27.20, 26.75, 24.88, 23.62, 22.98, 21.84, 14.39.

*4.5.3. 3-(4-(Hexyloxy)-1,2,5-thiadiazol-3-yl)-1-(12-((1,2,3,4-tetrahydroacridin-9-yl)amino)dodecyl)pyridin-1-ium bromide (**15c**)*

The title compound was prepared by reacting **13** (100 mg, 0.380 mmol) and **9c** (200 mg, 0.449 mmol) in DMF (10 mL). After standard workup, **15c** was obtained as a yellow oil (60 mg , 22%): $R_f$ = 0.26 (DCM/MeOH 9:1). $^1$H NMR (400 MHz, $CD_3OD$): *δ* 9.61 (s, 1H; H2′), 9.24 (dt, *J* = 8.3, 1.3, 1.2 Hz, 1H; H4′), 9.07 (d, *J* = 6.1 Hz, 1H; H6′), 8.39 (d, *J* = 8.3 Hz, 1H; H5′), 8.25 (dd, *J* = 8.1, 6.2 Hz, 1H; H9), 7.85 (ddd, *J* = 8.1, 6.9, 1.1 Hz, 1H; H6), 7.77 (dd, *J* = 8.5, 0.9 Hz, 1H; H7), 7.58 (ddd, *J* = 8.4, 6.9, 1.3 Hz, 1H; H8), 4.75 (t, *J* = 7.6 Hz, 2H; $CH_2$−$N^+$), 4.63 (t, *J* = 6.7 Hz, 2H; $CH_2$−O), 3.95 (t, *J* = 7.4 Hz, 2H; HN−C*H*$_2$), 3.02 (t, *J* = 5.6 Hz, 2H; H4), 2.71 (t, *J* = 5.4 Hz, 2H; H1), 2.09 (quint, *J* = 7.9 Hz, 2H; C*H*$_2$−$CH_2$−O), 2.01–1.92 (m, 6H; C*H*$_2$−$CH_2$−$N^+$, 2×H2, 2×H3), 1.83 (quint, *J* = 7.7 Hz, 2H; HN−$CH_2$−C*H*$_2$), 1.57–1.25 (m, 22H; HN−$(CH_2)_2$−C*H*$_2$−C*H*$_2$−C*H*$_2$−C*H*$_2$−C*H*$_2$−C*H*$_2$−C*H*$_2$−$(CH_2)_2$−$N^+$, $CH_3$−C*H*$_2$−C*H*$_2$−C*H*$_2$−$(CH_2)_2$−O), 0.93 (t, *J* = 7.1 Hz, 3H; C*H*$_3$−$(CH_2)_5$−O). $^{13}$C NMR (101 MHz, $CD_3OD$): *δ* 178.08, 164.50, 158.04, 151.69, 145.55, 144.15, 143.90, 141.86, 139.80, 134.12, 133.30, 129.67, 126.52, 126.31, 120.11, 117.07, 112.86, 73.35, 63.67, 49.07, 32.68, 32.50, 31.56, 30.64, 30.54, 30.35, 30.19, 29.90, 29.31, 27.75, 27.24, 26.79, 24.89, 23.65, 22.99, 22.95, 21.86, 14.38.

*4.6. General procedure for the synthesis of target compounds **7-Cn***

To a solution of intermediate pyridinium salt (**15**) (1 equiv) in MeOH (0.03 M), a solution of $NaBH_4$ (5 - 8 equiv) in MeOH (0.5 M) was added dropwise at 0°C, and the reaction was stirred for 5 h at room temperature. After quenching with a saturated solution of $NaHCO_3$, the aqueous phase was extracted with DCM. The pooled organic phases were dried over anhydrous $Na_2SO_4$ and concentrated under reduced pressure. The crude reaction mixtures were submitted to silica gel column chromatography (eluent: DCM/MeOH 95:5), providing the pure target derivatives **7-C8**, **7-C10** and **7-C12**.

*4.6.1. N-(8-(5-(4-(Hexyloxy)-1,2,5-thiadiazol-3-yl)-3,6-dihydropyridin-1(2H)-yl)octyl)-1,2,3,4-tetrahydroacridin-9-amine (**7-C8**)*

The title compound was prepared by reacting **15a** (100 mg, 0.153 mmol), and $NaBH_4$ (35 mg, 0.919 mmol) in 7 mL of MeOH. After standard workup, **7-C8** was obtained as a brown oil (21 mg, 24%): $R_f$ = 0.31 (DCM/MeOH 95:5). $^1$H NMR (400 MHz, $CD_3OD$): $\delta$ 8.38 (d, $J$ = 8.7 Hz, 1H; H9), 7.81 (dt, $J$ = 18.7, 7.9 Hz, 2H; H6, H7), 7.57 (dd, $J$ = 11.2, 4.3 Hz, 1H; H8), 7.14 (s, 1H; H4′), 4.47 (t, $J$ = 6.5 Hz, 2H; $CH_2$−O), 3.94 (t, $J$ = 7.3 Hz, 2H; HN−C$H_2$), 3.65 (s, 2H; H2′), 3.02 (d, $J$ = 5.7 Hz, 2H; H4), 2.83 (t, $J$ = 5.8 Hz, 2H; H1), 2.68 (dd, $J$ = 9.6, 6.4 Hz, 4H; 2×H6′, $CH_2$−N), 2.51 (d, $J$ = 3.7 Hz, 2H; H5′), 2.03–1.91 (m, 4H; 2×H2, 2×H3), 1.84 (dt, $J$ = 13.2, 6.5 Hz, 4H; C$H_2$−$CH_2$−O, HN−$CH_2$−C$H_2$), 1.65 (s, 2H; C$H_2$−$CH_2$−$CH_2$−O), 1.50–1.30 (m, 14H; HN−$(CH_2)_2$−C$H_2$−C$H_2$−C$H_2$−C$H_2$−$CH_2$−N, $CH_3$−C$H_2$−C$H_2$−$(CH_2)_3$−O), 0.92 (t, $J$ = 7.0 Hz, 3H; C$H_3$−$(CH_2)_5$−O). $^{13}$C NMR (101 MHz, $CD_3OD$): $\delta$ 163.81, 155.88, 154.84, 147.84, 143.32, 132.15, 129.90, 129.85, 127.30, 125.57, 123.55, 118.89, 114.49, 72.19, 59.46, 54.06, 50.35, 49.39, 32.56, 31.82, 31.44, 30.76, 30.42, 30.19, 29.89, 28.50, 27.71, 27.51, 26.82, 25.44, 23.61, 23.48, 22.67, 14.35. MS (ESI) *m/z* $[M+H]^+$ calcd for $C_{34}H_{50}BrN_5OS^+$: 575.37, found: 576.25. HPLC analysis: retention time = 8.275 min, purity 96.91%.

*4.6.2. N-(10-(5-(4-(Hexyloxy)-1,2,5-thiadiazol-3-yl)-3,6-dihydropyridin-1(2H)-yl)decyl)-1,2,3,4-tetrahydroacridin-9-amine (**7-C10**)*

The title compound was prepared by reacting **15b** (140 mg, 0.206 mmol), and $NaBH_4$ (474 mg, 1.066 mmol) in 9 mL of MeOH. After standard workup, **7-C10** was obtained as a brown oil (20 mg, 16%): $R_f$ = 0.41 (DCM/MeOH 95:5). $^1$H NMR (400 MHz, $CD_3OD$): $\delta$ 8.09 (d, $J$ = 8.6 Hz, 1H; H9), 7.66 (d, $J$ = 8.4 Hz, 1H; H6), 7.55 (t, $J$ = 7.6 Hz, 1H; H7), 7.33 (t, $J$ = 7.7 Hz, 1H; H8), 6.99 (t, $J$ = 3.8 Hz, 1H; H4′), 4.36 (t, $J$ = 6.4 Hz, 2H; $CH_2$−O), 3.57 (t, $J$ = 7.1 Hz, 2H; HN−C$H_2$), 3.38 (s, 2H; H2′), 2.89 (s, 2H; H4), 2.63 (s, 2H; H1), 2.55 (t, $J$ = 5.7 Hz, 2H; H6′), 2.45–2.37 (m, 2H; $CH_2$−N), 2.37–2.30 (m, 2H; H5′), 1.87–1.80 (m, 4H; 2×H2, 2×H3), 1.73 (quint, $J$ = 7.0 Hz, 2H; HN−$CH_2$−C$H_2$), 1.60 (d, $J$ = 7.2 Hz, 2H; C$H_2$−$CH_2$−O), 1.54–1.44 (m, 2H; C$H_2$−$CH_2$−$CH_2$−O), 1.43–1.12 (m, 18H; HN−$(CH_2)_2$−C$H_2$−C$H_2$−C$H_2$−C$H_2$−C$H_2$−C$H_2$−$CH_2$−N, $CH_3$−C$H_2$−C$H_2$−$(CH_2)_3$−O), 0.82 (t, $J$ = 7.0 Hz, 3H; C$H_3$−$(CH_2)_5$−O). $^{13}$C NMR (101 MHz, $CD_3OD$): $\delta$ 163.86, 156.60, 154.94, 147.93, 139.81, 133.93, 131.23, 130.00, 129.88, 125.24, 125.14, 119.91, 115.45, 72.20, 59.55, 54.09, 50.39, 49.56, 32.57, 32.01, 30.79, 30.75, 30.52, 30.45, 30.44, 30.25, 29.91, 28.63, 27.78, 27.58, 26.83, 25.72, 23.75, 23.61, 23.10, 14.32. MS (ESI) *m/z* $[M+H]^+$ calcd for $C_{36}H_{54}BrN_5OS^+$: 603.40, found: 604.25. HPLC analysis: retention time = 8.3 min, purity 96.7%.

*4.6.3. N-(12-(5-(4-(Hexyloxy)-1,2,5-thiadiazol-3-yl)-3,6-dihydropyridin-1(2H)-yl)dodecyl)-1,2,3,4-tetrahydroacridin-9-amine (**7-C12**)*

The title compound was prepared by reacting **15c** (200 mg, 0.282 mmol), and $NaBH_4$ (86 mg, 2.26 mmol) in 12 mL of MeOH. After standard workup, **7-C12** was obtained as a brown oil (84 mg, 47%): $R_f$ = 0.46 (DCM/MeOH 95:5). $^1$H NMR (400 MHz, $CD_3OD$): $\delta$ 8.35 (d, $J$ = 8.7 Hz, 1H; H9), 7.86–7.73 (m, 2H; H6, H7), 7.55 (ddd, $J$ = 8.5, 6.6, 1.6 Hz, 1H; H8), 7.11 (dd, $J$ = 3.7, 2.0 Hz, 1H; H4′), 4.46 (t, $J$ = 6.5 Hz, 2H; $CH_2$−O), 3.90 (t, $J$ = 7.2 Hz, 2H; HN−C$H_2$), 3.66–3.53 (m, 2H; H2′), 3.01 (s, 2H; H4), 2.78–2.65 (m, 4H; 2×H1, 2×H6′), 2.65–2.55 (m, 2H; $CH_2$−N), 2.48 (s, 2H; H5′),

1.96 (s, 4H; H2), 1.90–1.71 (m, 4H; 2×H3, HN−$CH_2$−C$H_2$), 1.69–156 (m, 2H; C$H_2$−$CH_2$−O), 1.56–1.14 (m, 24H; HN−$(CH_2)_2$−C$H_2$−C$H_2$−C$H_2$−C$H_2$−C$H_2$−C$H_2$−C$H_2$−C$H_2$−$CH_2$−N, $CH_3$−C$H_2$−C$H_2$−C$H_2$−$(CH_2)_2$−O), 0.92 (t, *J* = 7.0 Hz, 3H; C$H_3$−$(CH_2)_5$−O). $^{13}$C NMR (101 MHz, $CD_3OD$): *δ* 163.84, 157.47, 152.49, 147.66, 133.59, 129.75, 129.50, 127.33, 126.27, 126.11, 121.02, 117.55, 113.28, 72.24, 59.38, 53.83, 50.28, 49.24, 32.57, 31.59, 30.63, 30.60, 30.56, 30.53, 30.25, 29.90, 29.88, 28.57, 27.70, 27.36, 27.24, 26.82, 26.51, 25.01, 23.61, 23.13, 22.08, 14.34. MS (ESI) *m/z* $[M+H]^+$ calcd for $C_{38}H_{58}BrN_5OS^+$: 631.43, found: 632.35. HPLC analysis: retention time = 8.9 min, purity 95.7%.

### *4.7. General procedure for the synthesis of target compounds **8-Cn***

The reaction was conducted under Argon atmosphere. To a solution of Xanomeline **3** (1 equiv) in dry $CH_3CN$ (0.1 M) a solution of functionalized tacrine bromide (**9**) (1 equiv) in dry $CH_3CN$ (0.1 M) was added. The mixture was reacted for 10 h at 80 °C in a microwave apparatus (pressure: 19 atm, power of 500 W). The crude reaction mixtures were submitted to silica gel column chromatography (eluent: DCM/MeOH 99:1 → 9:1), providing the pure target derivatives **8-C8**, **8-C10** and **8-C12**.

#### *4.7.1. 5-(4-(Hexyloxy)-1,2,5-thiadiazol-3-yl)-1-methyl-1-(8-((1,2,3,4-tetrahydroacridin-9-yl)amino)octyl)-1,2,3,6-tetrahydropyridin-1-ium bromide (**8-C8**)*

The title compound was prepared by reacting **3** (150 mg, 0.533 mmol) and **9a** (228 mg, 0.586 mmol) in $CH_3CN$ (10 mL). After standard workup, **8-C8** was obtained as a beige solid (90 mg , 25%): $R_f$ = 0.36 (DCM/MeOH 9:1). mp = 96–98 °C. $^1$H NMR (400 MHz, $CD_3OD$): *δ* 8.43 (d, *J* = 8.7 Hz, 1H; H9), 7.87 (ddd, *J* = 8.5, 7.0, 1.1 Hz, 1H; H6), 7.81 (dd, *J* = 8.5, 1.2 Hz, 1H; H7), 7.61 (ddd, *J* = 8.4, 6.8, 1.4 Hz, 1H; H8), 7.32 (dd, *J* = 4.8, 3.3 Hz, 1H; H4′), 4.56–4.48 (m, 4H; $CH_2$−O, 2×H2′), 3.99 (d, *J* = 7.3 Hz, 2H; HN−C$H_2$), 3.72–3.62 (m, 2H; $CH_2$−$N^+$), 3.52 (t, *J* = 8.3 Hz, 2H; H6′), 3.21 (s, 3H; $CH_3$−$N^+$), 3.05 (t, *J* = 5.6 Hz, 2H; H4), 2.83 (s, 2H; H1), 2.74 (t, *J* = 5.4 Hz, 2H; H5′), 2.05–

1.80 (m, 10H; 2×H2, 2×H3, C*H*$_2$CH$_2$O, C*H*$_2$CH$_2$N$^+$, NHCH$_2$C*H*$_2$), 1.56–1.33 (m, 14H; HN−(CH$_2$)$_2$−C*H*$_2$−C*H*$_2$−C*H*$_2$−C*H*$_2$−(CH$_2$)$_2$−N$^+$, CH$_3$−C*H*$_2$−C*H*$_2$−C*H*$_2$−(CH$_2$)$_2$−O), 0.95 (t, *J* = 7.1 Hz, 3H; C*H*$_3$−(CH$_2$)$_5$−O). $^{13}$C NMR (101 MHz, CD$_3$OD): *δ* 163.94, 157.91, 151.69, 145.53, 139.82, 134.03, 127.67, 126.50, 126.29, 124.34, 120.17, 117.07, 112.87, 72.63, 65.60, 60.25, 57.26, 49,14, 48.37, 32.58, 31.53, 30.57, 30.28, 29.86, 29.38, 27.70, 27.42, 26.75, 24.97, 23.59, 23.12, 23.00, 22.60, 21.87, 14.37. MS (ESI) *m/z* [M+H]$^+$ calcd for C$_{35}$H$_{53}$BrN$_5$OS$^+$: 590,39, found: 590.25. HPLC analysis: retention time = 8.2 min, purity 97.8%.

### *4.7.2. 5-(4-(Hexyloxy)-1,2,5-thiadiazol-3-yl)-1-methyl-1-(10-((1,2,3,4-tetrahydroacridin-9-yl)amino)decyl)-1,2,3,6-tetrahydropyridin-1-ium bromide (**8-C10**)*

The title compound was prepared by reacting **3** (140 mg, 0.497 mmol) and **9b** (270 mg, 0.647 mmol) in CH$_3$CN (10 mL). After standard workup, **8-C10** was obtained as a yellow oil (135 mg, 39%): $R_f$ = 0.42 (DCM/MeOH 9:1). $^1$H NMR (400 MHz, CD$_3$OD): *δ* 8.40 (d, *J* = 8.7 Hz, 1H; H9), 7.85 (ddd, *J* = 8.4, 7.0, 1.1 Hz, 1H; H6), 7.79 (d, *J* = 7.6 Hz, 1H; H7), 7.59 (ddd, *J* = 8.4, 6.8, 1.3 Hz, 1H; H8), 7.30 (t, *J* = 4.0 Hz, 1H; H4′), 4.53–4.48 (m, 4H; CH$_2$−O, 2×H2′), 3.96 (t, *J* = 7.3 Hz, 2H; HN−C*H*$_2$), 3.71–3.61 (m, 2H; CH$_2$−N$^+$), 3.49 (t, *J* = 8.0 Hz, 2H; H6′), 3.19 (s, 3H; CH$_3$−N$^+$), 3.03 (t, *J* = 5.5 Hz, 2H; H4), 2.81 (s, 2H; H1), 2.72 (t, *J* = 5.3 Hz, 2H; H5′), 2.01–1.80 (m, 10H; 2×H2, 2×H3, C*H*$_2$CH$_2$O, C*H*$_2$CH$_2$N$^+$, NHCH$_2$C*H*$_2$), 1.53–1.28 (m, 18H HN−(CH$_2$)$_2$−C*H*$_2$−C*H*$_2$−C*H*$_2$−C*H*$_2$−C*H*$_2$−C*H*$_2$−(CH$_2$)$_2$−N$^+$, CH$_3$−C*H*$_2$−C*H*$_2$−C*H*$_2$−(CH$_2$)$_2$−O), 0.93 (t, *J* = 7.1 Hz, 3H; C*H*$_3$−(CH$_2$)$_5$−O). $^{13}$C NMR (101 MHz, CD$_3$OD): *δ* 163.97, 158.00, 151.67, 145.54, 139.79, 134.09, 127.67, 126.54, 126.33, 124.36, 120.10, 117.07, 112.86, 72.65, 65.63, 60.27, 57.28, 49.28, 49.14, 32.58, 31.54, 30.44, 30.39, 30.26, 30.15, 29.86, 29.34, 27.71, 27.41, 26.75, 24.95, 23.59, 23.12, 22.99, 22.59, 21.86, 14.34. MS (ESI) *m/z* [M+H]$^+$ calcd for C$_{37}$H$_{57}$BrN$_5$OS$^+$: 618.42, found: 618.30. HPLC analysis: retention time = 8.6 min, purity 97.3%.

*4.7.3. 5-(4-(Hexyloxy)-1,2,5-thiadiazol-3-yl)-1-methyl-1-(12-((1,2,3,4-tetrahydroacridin-9-yl)amino)dodecyl)-1,2,3,6-tetrahydropyridin-1-ium bromide (**8-C12**)*

The title compound was prepared by reacting **3** (150 mg, 0.533 mmol) and **9c** (237 mg, 0.533 mmol) in $CH_3CN$ (10 mL). After standard workup, **8-C12** was obtained as a beige solid (115 mg , 30%): $R_f$ = 0.54 (DCM/MeOH 9:1). mp = 93–96 °C. $^1$H NMR (400 MHz, $CD_3OD$): $\delta$ 8.40 (d, $J$ = 8.7 Hz, 1H; H9), 7.88–7.78 (m, 2H; H6, H7), 7.58 (ddd, $J$ = 8.4, 6.6, 1.5 Hz, 1H; H8), 7.29 (t, $J$ = 3.9 Hz, 1H; H4′), 4.56–4.45 (m, 4H; $CH_2$−O, 2×H2′), 3.95 (t, $J$ = 7.3 Hz, 2H; HN−C$H_2$), 3.74–3.59 (m, 2H; $CH_2$−$N^+$), 3.51 (t, $J$ = 7.8 Hz, 2H; H6′), 3.20 (s, 3H; $CH_3$−$N^+$), 3.03 (t, $J$ = 5.6 Hz, 2H; H4), 2.82 (s, 2H; H1), 2.71 (t, $J$ = 5.4 Hz, 2H; H5′), 2.04–1.78 (m, 10H; 2×H2, 2×H3, C$H_2$$CH_2$O, C$H_2$$CH_2$$N^+$, NH$CH_2$C$H_2$), 1.54–1.22 (m, 22H HN−$(CH_2)_2$−C$H_2$−C$H_2$−C$H_2$−C$H_2$−C$H_2$−C$H_2$−C$H_2$−$(CH_2)_2$−$N^+$, $CH_3$−C$H_2$−C$H_2$−C$H_2$−$(CH_2)_2$−O), 0.92 (t, $J$ = 7.0 Hz, 3H; C$H_3$−$(CH_2)_5$−O). $^{13}$C NMR (101 MHz, $CD_3OD$): $\delta$ 163.94, 157.90, 151.69, 145.54, 139.80, 134.03, 127.69, 126.50, 126.30, 124.34, 120.16, 117.06, 112.86, 72.63, 65.61, 60.25, 57.27, 49,27, 49.13, 32.57, 31.52, 30.55, 30.48, 30.26, 30.18, 29.85, 29.38, 27.68, 27.41, 26.74, 24.98, 23.57, 23.12, 22.99, 22.60, 21.86, 14.35. MS (ESI) *m/z* $[M+H]^+$ calcd for $C_{40}H_{62}BrN_5OS^+$: 646.45, found: 646.30. HPLC analysis: retention time = 8.9 min, purity 96.8%.

*4.8. Biology*

The Chinese hamster ovary (CHO) cell line stably expressing $hM_1$ receptor was obtained from Wyeth Research (Princeton, NJ). 384-well microplates and white 96-well plates were purchased from Thermo Fisher and Greiner Bio One, Germany, respectively. Dulbecco's modified Eagle's medium (DMEM) and phosphate-buffered saline (PBS) were from Sigma (Germany). Leibovitz's L-15 medium (L-15) and Hank's balanced salt solution (HBSS) were from Gibco (Germany). Fetal calf serum (FCS), trypsin and geneticin (G418) were from Merck Biochrom (Germany). D-Luciferin was

purchased as potassium salt from Pierce (Germany) and was dissolved in HBSS at a 400 mM concentration. Puromycin was obtained from Invivogen (France).

### *4.8.1. Inhibition of Acetylcholinesterase*

AChE (E.C. 3.1.1.7, from electric eel) was purchased from Sigma Aldrich (Steinheim, Germany). 5,5'-Dithiobis-(2-nitrobenzoic acid) (DTNB or Ellman's reagent) and acetylthiocholine iodide (ATC) were obtained from Fluka (Buchs, Switzerland). For buffer preparation, 2.40 g of potassium dihydrogen phosphate were dissolved in 500 mL of water and adjusted to pH 8.0 with a NaOH solution (0.1 M). Enzyme solutions were prepared with buffer to give 2.5 units per mL and stabilized with 2 mg bovine serum albumin (SERVA, Heidelberg, Germany) per mL of enzyme solution. 396 mg of DTNB were dissolved in 100 mL of buffer to give a 10 mM solution (0.3 mM in assay). The stock solutions of the test compounds were prepared either in pure buffer or, if insoluble, in pure ethanol with a concentration of 33.3 mM (1 mM in assay) and diluted stepwise with ethanol to a concentration of 33.3 nM (1 nM in assay). The highest concentration of the test compounds applied in the assay was $10^{-3}$ M (the amount of EtOH in the stock solution did not influence the enzyme activity in the assay). The assay was performed at 25 °C according to a previously described protocol [3]. Spectrophotometric measurements were performed on a Shimadzu UVmini-1240 spectrophotometer (Duisburg, Germany) at 412 nm.

### *4.8.2. Cell cultures*

Chinese hamster ovary (CHO) cells stably expressing the $hM_1$ receptor (CHO-$hM_1$ cells) were cultured in Ham's nutrient mixture F-12 (HAM- F12) supplemented with 10 % (v/v) FCS, 100 U/mL penicillin, 100 µg/mL streptomycin, 0.2 mg/mL G418 and 2 mM L-glutamine at 37°C in a 5 % $CO_2$ humidified atmosphere. The HEK293T cells stably co-transfected with the human $M_1$ receptor and the $G\alpha_q$-PLC-β3 sensor were kindly provided by Timo Littmann (University of Regensburg). Cells

were cultivated in DMEM containing 10% FCS (full medium) at 37 °C in a water-saturated atmosphere containing 5% $CO_2$ as previously reported [35].

*4.8.3. Split Luciferase bioluminescence assay*

In brief, cells were detached from a 75-$cm^2$ flask by trypsinization and centrifuged (700 × *g* for 5 min). The pellet was resuspended in the assay medium consisting of L-15 with 5% FCS and the density of the suspension was adjusted to $1.25 \cdot 10^6$ cells/mL. Then, 80 µL of this suspension were seeded into each well of a 96-well plate, and the plate was incubated at 37 °C in a humidified atmosphere (without additional $CO_2$) overnight. On the next day, 10 µL of 10 mM D-Luciferin were added to the cells, and the plate was transferred into a pre-warmed microplate luminescence reader (Mithras LB 940 Multimode Microplate Reader, Berthold Technologies). The cells were allowed to equilibrate inside the reader for 10 min before the basal luminescence was determined by recording the luminescence for the entire plate ten times with an integration time of 0.5 s per well. In the meantime, serial dilutions of agonists were prepared. The resulting solutions were also pre-warmed to 37 °C and subsequently added to the cells. Thereafter, luminescence was recorded for 15 plate repeats amounting to a time period of 20 min. Negative controls (solvent) and positive controls (reference full agonist, carbachol ($hM_1R$), eliciting a maximal 100 % response) were included for subsequent normalization of the data. When the antagonist mode was evaluated, antagonists were added 15 min prior to the initial thermal equilibration period, to ensure their equilibrium with the receptors before adding the agonists. The p$K_b$ values of antagonists were determined according to the Cheng-Prusoff equation [44]. After data acquisition, the peak luminescence intensities obtained after stimulation were used for quantitative analysis using the Graph Pad Software, San Diego, CA. The $hM_1R$ construct was kindly provided by Timo Littmann (University of Regensburg).

*4.8.4. IP-One accumulation assay*

In brief, CHO-$hM_1$ cells were grown to a confluence of about 80%, were detached from the culture dish, resuspended in assay buffer (HEPES, 10 mM, $CaCl_2$, 1 mM, $MgCl_2$, 0.5 mM, KCl, 4.2 mM, NaCl, 146 mM, glucose, 5.5 mM, LiCl, 50 mM, pH 7.4), counted using the Neubauer counting chamber and dispensed in 384-well microplates at a density of $1\times10^7$cells/mL. After incubation with the test compounds dissolved in stimulation buffer at 37 °C for 30 min, the detection reagents were added (IP1-d2 conjugate and Anti-IP1cryptate TB conjugate, each dissolved in lysis buffer), and incubation was maintained at room temperature for 60 min. Time-resolved fluorescence resonance energy transfer (HTRF) was determined after excitation at 320 nm using the Wallac EnVision 2104 Multilabel plate reader. Data analysis was based on the fluorescence ratio emitted by labeled IP1 (665 ± 10 nm) over the light emitted by the europium cryptate-labeled anti-IP1 (615 ± 10 nm). Levels of IP1 were normalized to the amount generated in the presence of 100 µM ACh. All compounds were tested in triplicate in at least three individual experiments.

#### *4.8.5. Data processing*

Data are shown as means ± S.E.M. for n independent experiments. Statistical analysis and curve fitting were performed using Prism 5.01 (GraphPad Software, San Diego, CA). In the Ellman's assay, the percentage of enzyme activity was plotted against the logarithm of the compound concentrations from which the $IC_{50}$ values were calculated. Data of the IP1 accumulation assay were processed by plotting the ratios (emission at 665 nm/emission at 615 nm) of the HTRF measurements against log (concentration of compounds) and analyzed by a four-parameter logistic equation (log(agonist) vs. response - variable slope) (GraphPad Software, San Diego, CA), followed by normalization using CCh as reference compound.

### *4.9. Computational analysis*

The docking studies followed a previously developed protocol for tacrine-based bivalent compounds [45], with slight adaptation of search parameters to improve convergence in the present

case. The protein structure was prepared from the high-resolution crystal structure of *Torpedo californica* AChE (TcAChE) complexed with a bis-tacrine compound (PDB 2CKM) [46]. The continuously resolved polypeptide chain from Ser4 to Pro485 of this PDB structure was used for docking after removing two *N*-acetyl-glucosamine residues and all water molecules and adding missing side chain atoms. Protein and ligand preparations were carried out with the Molecular Operating Environment (MOE) 2018.01 [47]. Protonation states were set according to the expected ionization at pH 8 (corresponding to Ellman assay conditions), which resulted in a protonated tacrine moiety. The ligand structures were built in MOE (using the S-configuration for the methylated **8-Cn** hybrids) and energy minimized with the MMFF94x force field to an rms-gradient of 0.001 kcal/(mol·Å).

Docking calculations were carried out with GOLD v5.2.2 [48.49], using the Astex Statistical Potentials (ASP) as scoring function. Each ligand was subjected to 50 independent runs, with the number of operations set to 4.000.000 per run. Due to the large conformational flexibility of the compounds, the search parameters of the genetic algorithm were adjusted with respect to population size (500), crossover frequency (90) and migration frequency (20). Following the previous approach of Chen et al. [45] and Messerer et al. [3], a scaffold match constraint was applied to place the tacrine moiety in the catalytic active site as observed in the crystal structures. Unconstrained docking supported the feasibility of the placement of the tacrine moiety (results not shown). The 50 docking poses obtained from GOLD were clustered with respect to binding-mode similarity, using a root-mean-square-deviation (RMSD) of 2 Å as cutoff, and re-scored with DrugScoreX (DSX) based on CSD potentials [50]. The before discussed representative docking solutions were obtained from the best-ranked cluster containing at least 10 poses by selecting the pose with the best consensus score from DSX and ASP. The PyMOL Molecular Graphics System v2.2.3 was used for visual analysis and figure preparation [51].

**Acknowledgments**

Special thanks are due to Timo Littmann for the generous gift of the cells expressing the Split-Luc construct. D.V. received financial support by the international doctoral college “Receptor Dynamics: Emerging Paradigms for Novel Drugs” funded within the framework of the Elite Network of Bavaria (ENB). (Grant number K-BM-2013-247). N.Y.C. was supported by a fellowship of the Bavarian Ministry for Science and Arts. The PhD position of M.M. is financed by the University of Milan.

## Declaration of Competing Interest

The authors declared that they have no conflicts of interest.

## Appendix A. Supplementary material

Supplementary data to this article can be found online.

## References

[1] S. Verma, A. Kumar, T. Tripathi, A. Kumar, Muscarinic and nicotinic acetylcholine receptor agonists: current scenario in Alzheimer's disease therapy, J. Pharm. Pharmacol. 70 (2018) 985–993.

[2] E. Scarpini, P. Scheltens, H. Feldman, Treatment of Alzheimer's disease: current status and new perspectives, Lancet Neurol. 2 (2003) 539–547.

[3] R. Messerer, C. Dallanoce, C. Matera, S. Wehle, L. Flammini, B. Chirinda, A. Bock, M. Irmen, C. Tränkle, E. Barocelli, M. Decker, C. Sotriffer, M. De Amici, U. Holzgrabe, Novel bipharmacophoric inhibitors of the cholinesterases with affinity to the muscarinic receptors $M_1$ and $M_2$, Med. Chem. Commun. 8 (2017) 1346–1359.

[4] P.B. Watkins, H.J. Zimmerman, M.J. Knapp, S.I. Gracon, K.W. Lewis, Hepatotoxic effects of tacrine administration in patients with Alzheimer's disease, J. Amer. Med. Ass. 271 (1994) 992–998.

[5] L. Fang, S. Jumpertz, Y. Zhang, D. Appenroth, C. Fleck, K. Mohr, C. Tränkle, M. Decker, Hybrid molecules from xanomeline and tacrine: Enhanced tacrine actions on cholinesterases and muscarinic $M_1$ receptors, J. Med. Chem. 53 (2010) 2094–2103.

[6] J.S. Kiefer-Day, H.E. Campbell, J. Towles, E.E. El-Fakahany, Muscarinic subtype selectivity of thetrahydroaminoacridine: Possible relationship to its capricious efficacy, Eur. J. Pharmacol. 203 (1991) 421–423.

[7] J.H.M. Lange, H.K.A.C. Coolen, M.A.W. van der Neut, A.J.M. Borst, B. Stork, P.C. Verveer, C.G. Kruse, Design, synthesis, biological properties, and molecular modeling investigations of novel tacrine derivatives with a combination of acetylcholinesterase inhibition and cannabinoid $CB_1$ receptor antagonism, J. Med. Chem. 53 (2010) 1338–1346.

[8] X. Chen, K. Zenger, A. Lupp, B. Kling, J. Heilmann, C. Fleck, B. Kraus, M. Decker, Tacrine-silibinin codrug shows neuro- and hepatoprotective effects *in vitro* and pro-cognitive and hepatoprotective effects *in vivo*. J. Med. Chem. 55 (2012) 5231–5242.

[9] M.C. Carreiras, E. Soriano, J.L. Marco, Multipotent 1,8-naphthyridines, as new tacrine analogues, for the treatment of Alzheimer's disease, in: K.L. Ameta, R.P. Pawar, A.J. Domb (Eds.), Bioactive Heterocycles: Synthesis and Biological Evaluation, Nova Science Publisher, New York, 2013, pp. 1–18.

[10] A. Romero, R. Cacabelos, M.J. Oset-Gasque, A. Samadi, J. Marco-Contelles, Novel tacrine-related drugs as potential candidates for the treatment of Alzheimer's disease, Bioorg. Med. Chem. Lett. 23 (2013) 1916–1922.

[11] C. Galdeano, N. Coquelle, M. Cieslikiewicz-Bouet, M. Bartolini, B. Pérez, M.V. Clos, I. Silman, L. Jean, J.-P. Colletier, P.-Y. Renard, D. Muñoz-Torrero, Increasing polarity in tacrine and huprine derivatives: Potent anticholinesterase agents for the treatment of myasthenia gravis, Molecules 22 (2018) 634. doi:10.3390/molecules23030634

[12] M.L. Bolognesi, M. Bartolini, A. Tarozzi, F. Morroni, F. Lizzi, A. Milelli, A. Minarini, M. Rosini, P. Hrelia, V. Andrisano, C. Melchiorre, Multitargeted drugs discovery: Balancing anti-amyloid and anticholinesterase capacity in a single chemical entity, Bioorg. Med. Chem. Lett. 21 (2011) 2655–2658.

[13] E. Uliassi, F. Prati, S. Bongarzone, M.L. Bolognesi, Medicinal chemistry of hybrids for neurodegenerative diseases, in: M. Decker (Ed.), Design of Hybrid Molecules for Drug Development, 1st Edition, Elsevier, Amsterdam, 2017, pp. 259–277.

[14] Y.-P. Pang, F. Hong, P. Quiram, T. Jelacic, S. Brimijoin, Synthesis of alkylene linked bis-THA and alkylene linked benzyl-THA as highly potent and selective inhibitors and molecular probes of acetylcholinesterase, J. Chem. Soc. Perkin Trans. 1 (1997) 171–176.

[15] S.G. Anagnostaras, G.G. Murphy, S.E. Hamilton, S.L. Mitchell, N.P. Rahnama, N.M. Nathanson, A.J. Silva, Selective cognitive dysfunction in acetylcholine $M_1$ muscarinic receptor mutant mice, Nat. Neurosci. 6 (2003) 51–58.

[16] S. Jiang, Y. Li, C. Zhang, Y. Zhao, G. Bu, H. Xu, Y.-W. Zhang, $M_1$ muscarinic acetylcholine receptor in Alzheimer's disease, Neurosci. Bull. 30 (2014) 295–307.

[17] P.J. Conn, C.K. Jones, C.W. Lindsley, Subtype-selective allosteric modulators of muscarinic receptors for the treatment of CNS disorders, Trends Pharmacol. Sci. 30 (2009) 148–155.

[18] A.M. Bender, C.K. Jones, C.W. Lindsley, Classics in Chemical Neuroscience: Xanomeline, ACS Chem. Neurosci. 8 (2017) 435–443.

[19] A. Christopoulos, T.L. Pierce, J. L. Sorman, E.E. El-Fakahany, On the unique binding and activating properties of xanomeline at the $M_1$ muscarinic acetylcholine receptor, Mol. Pharmacol. 53 (1998) 1120–1130.

[20] B.E. Kane, M.K.O. Grant, E.E. El-Fakahany, D.M. Ferguson, Synthesis and evaluation of xanomeline analogs - Probing the wash-resistant phenomenon at the $M_1$ muscarinic acetylcholine receptor, Bioorg. Med. Chem. 16 (2008) 1376–1392.

[21] J. Jakubík, S. Tuček, E.E. El-Fakahany, Role of receptor protein and membrane lipids in xanomeline wash-resistant binding to muscarinic $M_1$ receptors. J. Pharmacol. Exp. Ther. 308 (2004) 105–110.

[22] T. Disingrini, M. Muth, C. Dallanoce, E. Barocelli, S. Bertoni, K. Kellershohn, K. Mohr, M. De Amici, U. Holzgrabe, Design, synthesis, and action of oxotremorine-related hybrid-type allosteric modulators of muscarinic acetylcholine receptors, J. Med. Chem. 49 (2006) 366–372.

[23] J. Antony, K. Kellershohn, M. Mohr-Andrä, A. Kebig, S. Prilla, M. Muth, E. Heller, T. Disingrini, C. Dallanoce, S. Bertoni, J. Schrobang, C. Tränkle, E. Kostenis, A. Christopoulos, H.-D. Höltje, E. Barocelli, M. De Amici, U. Holzgrabe, K. Mohr, Dualsteric GPCR targeting: A novel route to binding and signaling pathway selectivity, FASEB J. 23 (2009) 442–450.

[24] A. Bock, N. Merten, R. Schrage, C. Dallanoce, J. Batz, J. Klöckner, J. Schmitz, C. Matera, K. Simon, A Kebig, L. Peters, A. Muller, J. Schrobang-Ley, C. Tränkle, C. Hoffmann, M. De Amici, U. Holzgrabe, E. Kostenis, K. Mohr, The allosteric vestibule of a seven transmembrane helical receptor controls G-protein coupling, Nat. Commun. 3 (2012) 1044.

[25] C. Matera, L. Flammini, M. Quadri, V. Vivo, V. Ballabeni, U. Holzgrabe, K. Mohr, M. De Amici, E. Barocelli, S. Bertoni, C. Dallanoce, Bis(ammonio)alkane-type agonists of muscarinic acetylcholine receptors: Synthesis, *in vitro* functional characterization, and *in vivo* evaluation of their analgesic activity, Eur. J. Med. Chem. 75 (2014) 222–232.

[26] A. Bock, M. Bermudez, F. Krebs, C. Matera, B. Chirinda, D. Sydow, C. Dallanoce, U. Holzgrabe, M. De Amici, M.J. Lohse, G. Wolber, K. Mohr, Ligand binding ensembles determine graded agonist efficacies at a G protein-coupled receptor, J. Biol. Chem. 291 (2016) 16375–16389.

[27] R. Messerer, Synthesis of dualsteric ligands for muscarinic acetylcholine receptors and cholinesterase inhibitors, Doctoral Thesis, Universität Würzburg 2017, urn:nbn:de:bvb:20-opus-149007

[28] R. Messerer, M. Kauk, D. Volpato, M.C. Alonso Canizal, J. Klöckner, U. Zabel, S. Nuber, C. Hoffmann, U. Holzgrabe, FRET studies of quinolone-based bitopic ligands and their structural analogues at the muscarinic $M_1$ receptor, ACS Chem. Biol. 12 (2017) 833–843.

[29] E. Barocelli, V. Ballabeni, S. Bertoni, C. Dallanoce, M. De Amici, C. De Micheli, M. Impicciatore, New analogues of oxotremorine and oxotremorine-M: Estimation of their *in vitro* affinity and efficacy at muscarinic receptor subtypes, Life Sci. 67 (2000) 717–723.

[30] R. Schrage, W.K. Seemann, J. Klöckner, C. Dallanoce, K. Racké, E. Kostenis, M. De Amici, U. Holzgrabe, K. Mohr, Agonist with supraphysiological efficacy at the muscarinic $M_2$ acetylcholine receptor, Br. J. Pharmacol. 169 (2013) 357–370.

[31] S.-S. Xie, X.-B. Wang, J.-Y. Li, L. Yang, L.-Y. Kong, Design, synthesis and evaluation of novel tacrine-coumarin hybrids as multifunctional cholinesterase inhibitors against Alzheimer's disease, Eur. J. Med. Chem. 64 (2013) 540–553.

[32] Y. Sun, J. Chen, X. Chen, L. Huang, X. Li, Inhibition of cholinesterase and monoamine oxidase-B activity by tacrine-homoisoflavonoid hybrids, Bioorg. Med. Chem. 21 (2013) 7406–7417.

[33] P. Sauerberg, P.H. Olesen, S. Nielsen, S. Treppendahl, M.J. Sheardown, T. Honore, C.H. Mitch, J.S. Ward, A.J. Pike, Novel functional $M_1$ selective muscarinic agonists. Synthesis and structure-activity relationships of 3-(1,2,5-thiadiazolyl)-1,2,5,6-tetrahydro-1-methylpyridines, J. Med. Chem. 35 (1992) 2274–2283.

[34] G.L. Ellman, K.D. Courtney, V. Andres, R.M. Featherstone, A new and rapid colorimetric determination of acetylcholinesterase activity, Biochem. Pharmacol. 7 (1961) 88–95.

[35] T. Littmann, T. Ozawa, C. Hoffmann, A. Buschauer, G. Bernhardt, A split luciferase-based probe for quantitative proximal determination of $G\alpha_q$ signalling in live cells, Sci. Rep. 8 (2018) 17179.

[36] A. Bock, B. Chirinda, F. Krebs, R. Messerer, J. Batz, M. Muth, C. Dallanoce, D. Klingenthal, C. Tränkle, C. Hoffmann, M. De Amici, U. Holzgrabe, E. Kostenis, K. Mohr, Dynamic ligand binding dictates partial agonism at a G protein-coupled receptor, Nat. Chem. Biol. 10 (2014) 18–20.

[37] X. Chen, J. Klöckner, J. Holze, C. Zimmermann, W.K. Seemann, R. Schrage, A. Bock, K. Mohr, C. Tränkle, U. Holzgrabe, M. Decker, Rational design of partial agonists for the muscarinic $M_1$ acetylcholine receptor, J. Med. Chem. 58 (2015) 560–576.

[38] A. Randáková, E. Dolejší, V. Rudajev, P. Zimčík, V. Doležal, E.E. El-Fakahany, J. Jakubík, Classical and atypical agonists activate $M_1$ muscarinic acetylcholine receptors through common mechanisms, Pharmacol. Res. 97 (2015) 27–39.

[39] E.T. van der Westhuizen, A. Spathis, E. Khajehali, M. Jörg, S.N. Mistry, B. Capuano, A.B. Tobin, P.M. Sexton, P.J. Scammells, C. Valant, A. Christopoulos, Assessment of the molecular mechanisms of action of novel 4-phenylpyridine-2-one and 6-phenylpyrimidin-4-one allosteric modulators at the $M_1$ muscarinic acetylcholine receptors, Mol. Pharmacol. 94 (2018) 770–773.

[40] A. Jean, J-L. Tardieu, M. Préaudat, F. Degorce, K. Undisz. Implementation of Cisbio's HTRF® $M_1$ muscarinic receptor related assays on CyBio liquid handling solutions for small and high throughput.

[41] E. Trinquet, M. Fink, H. Bazin, F. Grillet, F. Maurin, E. Bourrier, H. Ansanay, C. Leroy, A. Michaud, T. Durroux, D. Maurel, F. Malhaire, C. Goudet, J.P. Pin, M. Naval, O. Hernout, F. Chrétien, Y. Chapleur, G. Mathis. D-myo-inositol 1-phosphate as a surrogate of D-myo-inositol 1,4,5-tris phosphate to monitor G protein-coupled receptor activation, Anal. Biochem. 358 (2006) 126–135.

[42] E.H. Rydberg, B. Brumshtein, H.M. Greenblatt, D.M. Wong, D. Shaya, L.D. Williams, P.R. Carlier, Y.-P. Pang, I. Silman, J.L. Sussman, Complexes of alkylene-linked tacrine dimers with Torpedo californica acetylcholinesterase. J. Med. Chem. 49 (2006) 5491–5500.

[43] C. Bissantz, B. Kuhn, M. Stahl, A medicinal chemist's guide to molecular interactions, J. Med. Chem. 53 (2010) 5061–5084.

[44] Y.-C. Cheng, W.H. Prusoff, Relationship between the inhibition constant ($K_I$) and the concentration of inhibitor which causes 50 per cent Inhibition ($I_{50}$) of an enzymatic reaction, Biochem. Pharmacol. 22 (1973) 3099–3108.

[45] X. Chen, S. Wehle, N. Kuzmanovic, B. Merget, U. Holzgrabe, B. König, C.A. Sotriffer, M. Decker, Acetylcholinesterase inhibitors with photoswitchable inhibition of β-amyloid aggregation, ACS Chem. Neurosci. 5 (2014) 377–389.

[46] E.H. Rydberg, B. Brumshtein, H.M. Greenblatt, D.M. Wong, D. Shaya, L.D. Williams, P.R. Carlier, Y.-P. Pang, I. Silman, J.L. Sussman, Complexes of alkylene-linked tacrine dimers with Torpedo californica acetylcholinesterase, J. Med. Chem. 49 (2006) 5491–5500.

[47] Molecular Operating Environment (MOE), 2013.08; Chemical Computing Group ULC, 1010 Sherbooke St. West, Suite #910, Montreal, QC, Canada, H3A 2R7, 2019.

[48] M.L. Verdonk, J.C. Cole, M.J. Hartshorn, C.W. Murray, R.D. Taylor, Improved protein-ligand docking using GOLD, Proteins 52 (2003) 609–623.

[49] CCDCSoftware. GOLDSUITE v.5.2.2, www.ccdc.cam.ac.uk

[50] G. Neudert, G. Klebe, DSX: A knowledge-based scoring function for the assessment of protein-ligand complexes, J. Chem. Inf. Model. 51 (2011) 2731–2745.

[51] Schrödinger-LLC. The PyMOL Molecular Graphics System, version 2.2.3.